# INTERACTION OF NON-SATURATED SURFACE GRAVITY WAVES WITH INTERNAL WAVES

J. Alex Thomson

Physical Dynamics, Incorporated

Prepared for:

Rome Air Development Center
Advanced Research Projects Agency

October 1972

RADC-TR-72- 280
Technical Report
October 1972

# INTERACTION OF NON-SATURATED SURFACE GRAVITY WAVES WITH INTERNAL WAVES

Physical Dynamics, Incorporated

Sponsored by
Defense Advanced Research Projects Agency
ARPA Order No. 1649



Approved for public release;
distribution unlimited.

The views and conclusions contained in this document are those of the authors and should not be interpreted as necessarily representing the official policies, either expressed or implied, of the Advanced Research Projects Agency or the U. S. Government.



Rome Air Development Center
Air Force Systems Command
Griffiss Air Force Base, New York

UNCLASSIFIED
Security Classification

## DOCUMENT CONTROL DATA - R & D

*(Security classification of title, body of abstract and indexing annotation must be entered when the overall report is classified)*

1. ORIGINATING ACTIVITY *(Corporate author)*
Physical Dynamics, Inc.
P.O. Box 1069
Berkeley, California 94701

2a. REPORT SECURITY CLASSIFICATION
UNCLASSIFIED

2b. GROUP

3. REPORT TITLE

INTERACTION OF NON-SATURATED SURFACE GRAVITY WAVES WITH INTERNAL WAVES

4. DESCRIPTIVE NOTES *(Type of report and inclusive dates)*
Scientific Report

5. AUTHOR(S) *(First name, middle initial, last name)*

J. Alex Thomson
Bruce J. West

6. REPORT DATE
October 1972

7a. TOTAL NO. OF PAGES
98

7b. NO. OF REFS
13

8a. CONTRACT OR GRANT NO.
F30602-72-C-0494

b. PROJECT NO.
16490402

c. Program Code No. 2E20

d. ARPA Order 1649

9a. ORIGINATOR'S REPORT NUMBER(S)
PD 72-023

9b. OTHER REPORT NO(S) *(Any other numbers that may be assigned this report)*
RADC-TR-72-280

10. DISTRIBUTION STATEMENT

Approved for public release; distribution unlimited.

11. SUPPLEMENTARY NOTES Monitored by
Leonard Strauss (RADC/OSCE)
Griffiss AFB, New York 13441
(315)-330-3451

12. SPONSORING MILITARY ACTIVITY
Defense Advanced Research Projects Agency
1400 Wilson Blvd.
Arlington, Va. 22209

13. ABSTRACT

The interaction of surface gravity waves with non-dispersive internal waves is studied by solving the equations of motion in a coordinate system moving with the time independent surface current system induced by the internal wave. A range of surface wavelengths is found which is reflected by the current system (as seen in this coordinate system). In the ocean-fixed frame these waves are identified as waves which interact strongly with the internal waves and exchange energy with it. The effect on the surface wave pattern and the relation to surface slicks are discussed.



DD FORM 1 NOV 65 1473

UNCLASSIFIED
Security Classification

| 14. KEY WORDS | LINK A | | LINK B | | LINK C | |
|---|---|---|---|---|---|---|
| | ROLE | WT | ROLE | WT | ROLE | WT |
| OCEAN WAVES | | | | | | |
| INTERNAL WAVES | | | | | | |
| WAVE SPECTRA | | | | | | |

# INTERACTION OF NON-SATURATED SURFACE GRAVITY WAVES WITH INTERNAL WAVES

J. Alex Thomson
Bruce J. West

Contractor: Physical Dynamics, Incorporated
Contract Number: F30602-72-C-0494
Effective Date of Contract: 1 May 1972
Contract Expiration Date: 30 April 1973
Amount of Contract: $48,118.00
Program Code Number: 2E20

Principal Inveatigator: J. Alex Thomson
Phone: 415 848-3063

Project Engineer: Joseph J. Simons
Phone: 315 330-3451

Contract Engineer: Leonard Strauss
Phone: 315 330-4712



This research was supported by the
Advanced Research Projects Agency
of the Department of Defenae and
was monitored by Leonard Strauss
RADC (OCSE) GAFB, NY 13440 under
Contract F30602-72-C-0494.

## PUBLICATION REVIEW

This technical report has been reviewed and is approved.

RADC Project Engineer

RADC Contract Engineer

TABLE OF CONTENTS

## LIST OF FIGURES

LIST OF FIGURES - Cont'd

## 1. INTRODUCTION

It is known that the surface currents associated with travelling internal waves can be sufficiently intense to produce modifications of the surface wave structure that are visible both to the eye and to radar (Ziegenbein, 1970; Perry and Schimke, 1965; Polvani, 1972). In a series of measurements off San Diego, Lafond (1963; 1966) has shown that visible surface slicks, under certain wind conditions, move with the underlying train of internal waves. A later series of measurements at the same instrument platform has shown that these slicks are detectable with radar and exhibit phase correlation with the current pattern produced by the internal wave train (Polvani, 1972).

Two different mechanisms have been suggested as responsible for the coupling of internal waves to surface waves, one associated with changes in surface composition and the other a direct modification of wave structure. Lafond (1966) suggested that the divergence and convergence of the surface current over the leading and trailing portion of an internal wave maximum disperses or concentrates extant organic material on the surface in a way correlated with the internal wave phase. The resulting increase in the damping coefficient in the convergence zones reduces the amplitude of short wavelength gravity-capillary waves in these areas and changes the average wave slope and reflectivity.

A number of authors have noted the resonant effect that may be expected on a surface wave packet that travels at the same speed as the internal wave train (Hartle and Zachariason, 1969; Holliday, 1971; Rosen-

bluth, 1971; Phillips, 1971; Ko, 1972). Since, at resonance, the wave packet is able to travel great distances while remaining at the same phase point of the internal wave, the continuing interaction leads to a continuous energy transfer from the internal to the surface wave.

The theoretical models of the wave-current interaction may be divided into two broad categories, which we might characterize as space oriented (wave packets) or wavenumber oriented (modal).

The wave packet models (WKB, eikonal, ray theory) developed by Longuet-Higgins/Stewart (1961), Whitham (1966), Phillips (1966), Holliday (1971), Ko (1972), consider the surface as a superposition of a number of spatially-localized wave packets, each characterized by a characteristic wavenumber $k(x,t)$ and wave frequency $\omega(x,t)$. These packets move along trajectories defined by

$$\frac{d\vec{x}}{dt} = \frac{\partial \omega}{\partial \vec{k}}$$

$$\frac{d\vec{k}}{dt} = -\frac{\partial \omega}{\partial \vec{x}} \quad .$$

where the notation indicates gradients in $\vec{k}$ and $\vec{x}$-space respectively.

The mode-oriented models [Ball (1964), Hasselman (1967), Hartle/Zachariason (1969), Rosenbluth (1971)] describe the surface essentially as a superposition of various modes (sine waves for the unperturbed ocean) and concentrate their attention on the transfer of energy between modes. When applied to small amplitude waves, both treatments are equivalent since the requirements for validity of the WKB approximation are usually well satisfied for the waves of interest. However, the equivalence tends

to be obscured in development of computational models. In a modal description, spatial structure is bound up in the details of the phase relationships between different wavenumber modes. On the other hand, the wavenumber structure and spectrum is related to the details of the spatial correlation function in the wave packet description. Rosenbluth (1971) combines elements of both descriptions in a "full-wave" treatment of a linear wave interacting with a variable surface current and shows the equivalence between eigenmodes and wavepackets trapped over troughs of the internal wave.

A major difficulty arises in the application of these mechanisms to describe ocean wave spectra. The ocean surface under typical wind conditions is poorly described as a simple linear superposition of sine waves. On the contrary, the wave amplitudes and slopes are usually driven to the point where non-linearities are dominant in providing a saturation limiting of the wave heights. These effects manifest themselves in the appearance of sharp crested waves and wave breaking (white caps). In the present series of reports we will develop a description of the dynamical properties of ocean wave spectra involving a transport or relaxation equation. Here we write the rate of change of the mean or expected value of the wave height power spectrum in the form

$$\frac{d}{dt} F(\vec{x},\vec{k},t) = A(\vec{x},\vec{k})\ \nabla_{\vec{x}} U + \text{generation terms} - \text{loss terms.}$$

where F is assumed to depend on $(\vec{x},\vec{k},t)$ and $\nabla_{\vec{x}} U$ is the local time averaged surface current gradient. The detailed development and modeling of the var-

ious phenomena contributing to wave growth and decay will be discussed in subsequent reports. In the present report we wish to lay the groundwork for the discussion of the wave-current interaction and to review the physics of the interaction process. To do this we will discuss primarily a linear description of the ocean surface. Many of the non-linear effects coupling various waves together can be considered as interactions to various orders of different wave fields and can be understood within the context of a linear model in terms of the interaction of a linear wave with a prescribed current field. Thus, part of the motivation of the present work is to describe the resonant interaction of a surface wave with a moving current pattern and part to clarify some of the concepts that underlie the non-linear theory.

We consider the current produced near the ocean surface by a long wavelength internal wave propagating along a sharp thermocline at depth D (see Figure 1). For small percentage changes in the density across the interface ($\Delta\rho/\rho$), the currents and potential of the internal wave are

$$\phi^{(o)} \simeq \frac{A_o}{K} \cosh Ky \sin K(x - c_o t) \quad , \tag{1.1}$$

$$U_x^{(o)} \simeq A_o \cosh Ky \cos K(x - c_o t) \quad , \tag{1.2a}$$

and

$$U_y^{(o)} \simeq A_o \sinh Ky \sin K(x - c_o t) \quad , \tag{1.2b}$$

where $c_o$ is the phase velocity of the interfacial wave. The vertical velocity of the surface has been taken to be zero (valid in the limit $\Delta\rho/\rho \to 0$). In this paper we study the effect of this current [Equation (1.1)] on the motion and pattern of the small wavelength surface gravity waves.

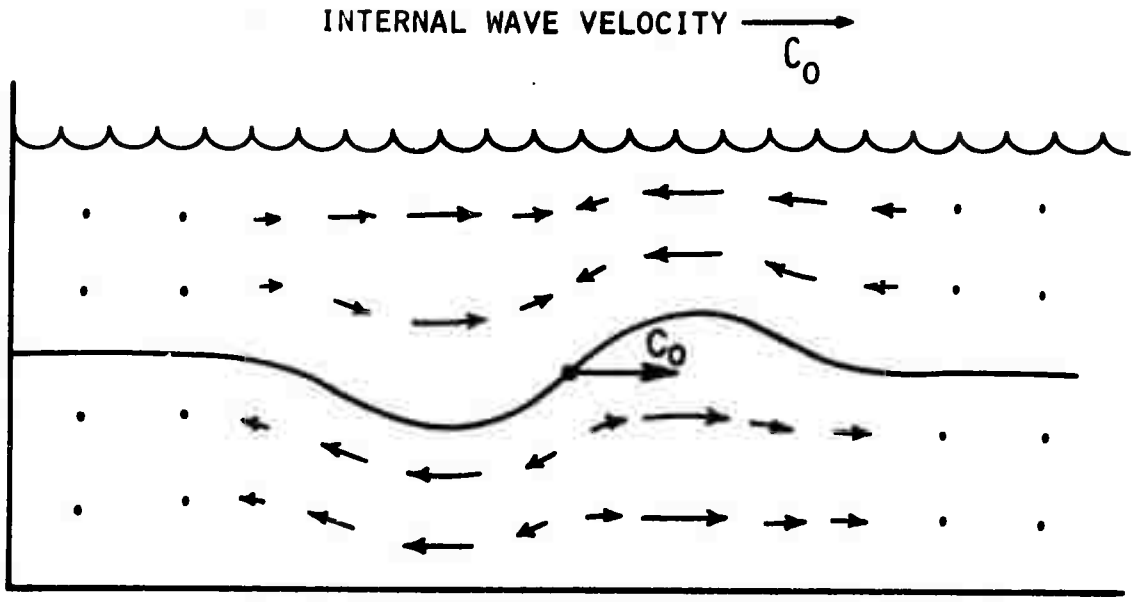


FIGURE 1A. CURRENTS IN THE OCEAN FIXED FRAME

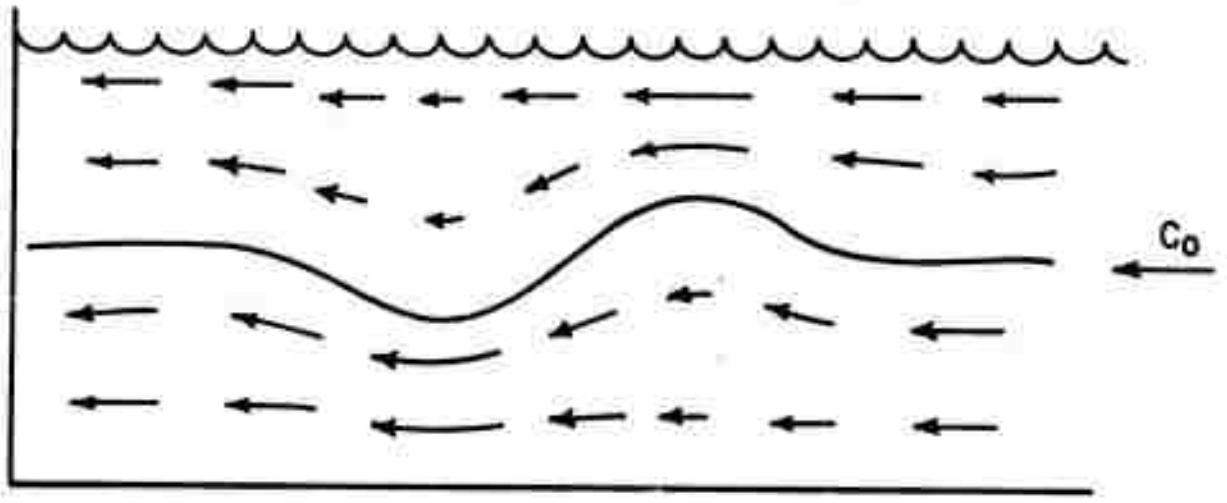


FIGURE 1B. CURRENTS IN THE INTERNAL WAVE FRAME

To get a feel for the basic physical versus the mathematical aspects involved in the problem, we examine first the dispersion relation for the surface waves for a uniform (deep)-ocean in the presence of a uniform current. It is well known that the dispersion relation in a coordinate system in which the ocean is stationary, has the form

$$\omega^2 = gk \tag{1.3}$$

or

$$\omega = \pm\sqrt{gk}$$

where $\omega$ is the angular wave frequency, k the wavenumber of the surface wave and g the gravitational acceleration. The velocity of a point of constant phase on the wave, i.e., phase velocity, is

$$c_{ph} = \frac{g}{\omega} = \pm\sqrt{g/k} \quad . \tag{1.4}$$

This dispersion relation is plotted in Figure 2a. Obviously, for each value of $|\omega|$ there are only two possible solutions and two wave velocities ($\pm\, g/|\omega|$) corresponding to waves travelling to the right or to the left.

If we now make a Galilean transformation to an observer moving over the ocean surface at velocity $c_o$, events appear to have a different time dependence. We must replace $\omega$ by $\omega + c_o k$ where $c_o$ is the observer velocity relative to the ocean. This has the tendency to twist the dispersion curves downward, i.e., the trajectory of the ocean surface, which was the real axis $\omega=0$, now becomes (see Fig. 2b)

$$\omega = - c_o k \quad . \tag{1.5}$$

This moving observer finds himself with a rather more complicated description of the same simple wave motion seen by the stationary observer. First he finds that there is a maximum frequency ($\omega^*$) above which waves will not propagate freely. At any lower frequency he finds that there are now four different wave-

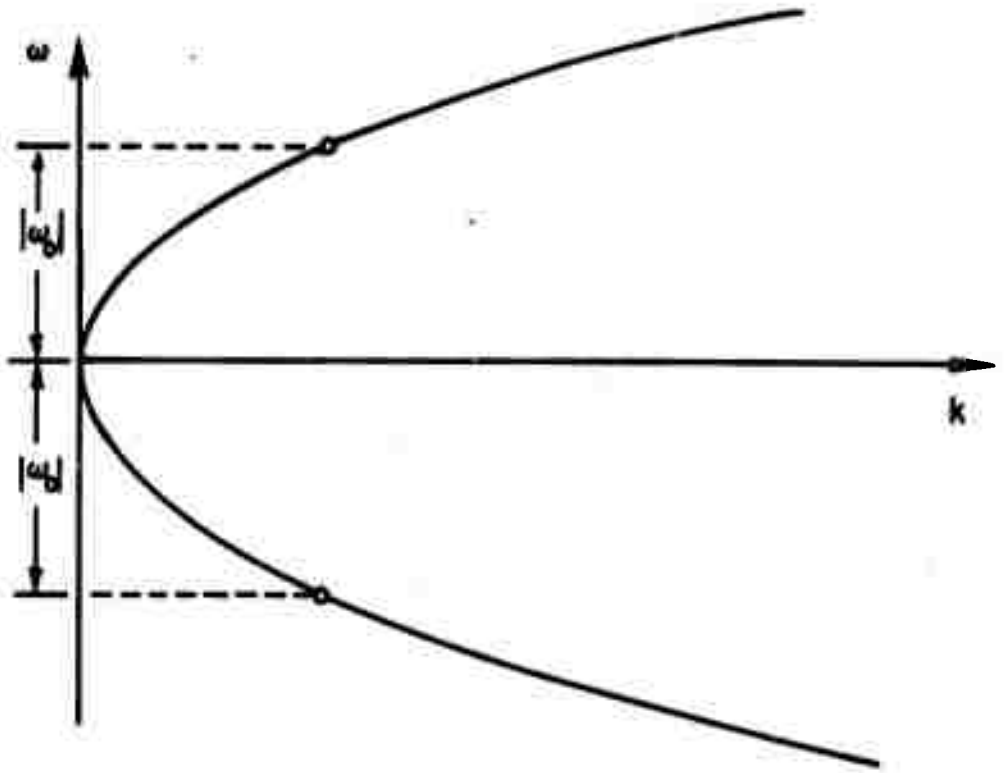


FIGURE 2A. DISPERSION RELATION IN THE OCEAN FRAME

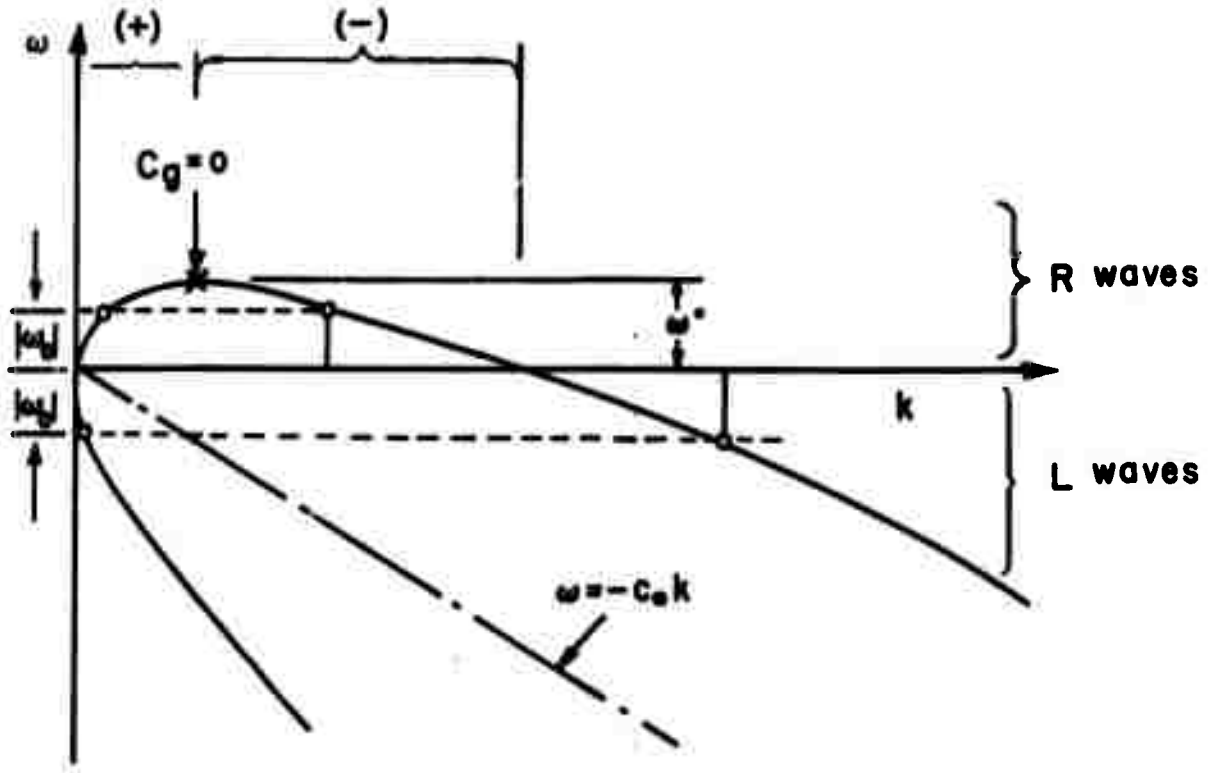


FIGURE 2B. DISPERSION RELATION IN A MOVING FRAME

numbers and wave velocities that will propagate freely for each given value of $|\omega|$ instead of two as in the ocean fixed frame. If this observer knew that in his coordinate system, the velocity of the ocean were locally uniform and independent of time, then he would correctly conclude that possible solutions have the form $\exp[-i\omega t + ikx]$ where there are two permissible right travelling waves ($\omega/k > 0$) and two left-travelling waves ($\omega/k < 0$) that are consistent with the same value of $|\omega|$.

All this is of little interest if the ocean current is truly independent of position since in that case the waves are simply manifestations of the two simple surface waves in Equ. (1.3). These two waves (or four depending on the coordinate system) are uncoupled and the transformation to a moving coordinate system merely complicates a simple problem. However, when the surface current varies with position (but not so rapidly as to invalidate the local validity of the dispersion relations) the problem is distinctly different. In the particular case of a travelling current disturbance there is a unique coordinate system in which the surface current distribution is independent of time. In this coordinate system, the solutions are harmonic in time ($e^{-i\omega t}$) but the spatial gradients may permit or induce coupling of the four waves.

Of particular interest are the two right travelling waves. Reference to Fig. 2b shows that, although the phase velocities for both are in the direction of the internal wave, the group velocities ($d\omega/dk$) have opposite signs. These two waves lie on either side of a turning point (where the group velocity vanishes). It will be shown in section 4 that a wave packet incident on a finite region of steady surface currents can be totally reflected for certain current patterns and that the two right travelling waves represent the incident and reflected wave trains. The observer in the ocean coordinate system would

interpret this reflection as follows. A surface gravity wave packet traveling at velocity $c_g$ (group) overtakes a traveling surface current region [translating at velocity $c(< c_g)$]. There will be a range of values for $c_g - c$, dependent on the maximum amplitude of the surface current, for which the gravity wave loses energy to the surface current to the extent that its propagation velocity is reduced to $2c - c_g$ [i.e., a velocity decrease of $2(c_g - c)$ because of reflection]. In the same manner, waves having group velocities less than but sufficiently close to surface current propagation velocity will be accelerated by the front edge of the moving current field to a velocity $c + (c - c_g)$. Thus, the surface current field acts as a piston to a certain range of wavelengths and pushes these waves along ahead of the current field. Waves near the condition $c = c_g$ will tend to pile up in front of or behind the reflection point and form caustics.

This type of interaction may be thought of as a resonance phenomenon where waves in a restricted range of frequencies interact strongly with the external forcing function. Indeed, in a modal description where the surface is represented as an assembly of harmonic oscillators, the reflection phenomena described above manifests itself specifically as a classical resonance interaction, between the oscillators (surface waves) and the external forcing function (internal wave).

In recent years considerable interest has been shown in this type of interaction and a number of treatments are available [Longuet-Higgins and Stewart (1960); Longuet-Higgins (1963); Ball (1964); Phillips (1966); Hasselman (1967); Hartle and Zachariason (1969); Rosenbluth (1972); Phillips (1972)]. The problem also has in interpretation in terms of parametric oscillator theory. In spite of this extensive analysis,

the relationships between the various methods are not readily transparent. Methods based on the WKB approximation allow trajectories of individual packets of energy to be followed. In available treatments, turning points can appear in the solutions where the WKB approximation fails (blockage effects, according to Phillips). Modal methods based on the Born approximation show a related singularity. The turning point here appears as an oscillator driven at resonance.

It is the purpose of this paper to analyze in detail the specific case of linear surface waves travelling on a spatially variable but steady current. The analysis is exact and, as a consequence, permits us to obtain bounded solutions in the neighborhood of the resonance region. By taking limiting cases of these exact solutions, we are able to demonstrate the relationships between the various more approximate models and, in particular, we are able to define their respective ranges of validity.

The details of these approaches are reviewed in the following section, along with an introduction to the present approach to the problem. In all cases, detailed theoretical analysis has been limited to a linear description of the interactions. Since the sea surface is usually in a strongly non-linear state, such approaches may have limited quantitative applicability. However, the linear analysis provides the insight necessary to the development of a non-linear theory.

The following sections segment the problem of internal and surface wave interactions as follows: Section 2 reviews some of the previous work done on the problem to familiarize the reader with the difficulties encountered and to point out where these studies left off. Section 3 provides an

introduction and review of scattering theory as it will be applied to the present problem. A set of coupled differential equations is constructed from an application of this theory under the assumption of a weakly reflecting current. These equations are then solved analytically for a linear current. Section 4 discusses solutions in both the Born and eikonal (WKB) approximations. These approximate solutions are then related to the results of Section 3. Section 5 summarizes the paper stressing the interconnection between the differing methods of approach and gives a physical interpretation to these methods. The connection with previous results and the interpretation of surface slicks in terms of reflected waves is also made.

## 2. COUPLED INTERNAL AND EXTERNAL WAVES (REVIEW)

We consider the wave motion at the surface of the ocean under the influence of a non-uniform surface current. In the analysis the ocean is assumed to be homogeneous and irrotational. Within this general framework, we may write the momentum equation for a fluid as

$$\frac{d\vec{u}}{dt} = -\frac{1}{\rho}\nabla p + \vec{g} \tag{2.1}$$

where, under the assumption of irrotational flow, $\nabla \times \vec{u} = 0$. The quantities in Eq. (2.1) are defined as follows: $\rho$ is the fluid density, $\vec{g}$ is the gravitational acceleration, $p$ is the pressure, and $\vec{u}$ is the velocity of the fluid. If we write $\vec{u} = \nabla\Phi$, where $\Phi$ is the potential description of the velocity field, then Eq. (2.1) may be written as

$$\frac{\partial\vec{u}}{\partial t} + \vec{u}\cdot\nabla\vec{u} = \nabla\left[\frac{\partial\Phi}{\partial t} + \frac{(\nabla\Phi)^2}{2}\right] = -\nabla\left\{\frac{p}{\rho} + gy\right\} \tag{2.2}$$

where the operator $d/dt$ in Eq. (2.1) has been replaced by the Eulerian derivative $\partial/\partial t + \vec{u}\cdot\nabla$ in Eq. (2.2) and the density has been assumed to be constant.

Equation (2.2) may be integrated immediately to yield the general equation

$$\Phi_t + \frac{1}{2}(\nabla\Phi)^2 + \frac{p}{\rho} + gy = f(t) \tag{2.3}$$

where in the following we set $f(t) = 0$.* At the surface of the fluid we will assume that the pressure is zero [$p = 0$, $y = y_s$, $\Phi = \Phi_s$], so that Eq. (2.3) becomes

$$\frac{\partial\Phi_s}{\partial t} + \frac{1}{2}(\nabla\Phi)_s^2 + gy_s = 0 \ . \tag{2.4}$$

* As required by the boundary condition at infinity that hydrostatic equilibrium prevail ($p = -\rho g y$).

This equation may be further modified by recalling that the rate of increase of $y_s$ following a fluid element is the vertical component of the fluid velocity:

$$\frac{dy_s}{dt} = \left(\frac{\partial \Phi}{\partial y}\right)_s \tag{2.5}$$

and that

$$\frac{d\Phi}{dt} = \frac{\partial \Phi}{\partial t} + \nabla\Phi \cdot \nabla\Phi \quad . \tag{2.6}$$

Introducing Equations (2.5) and (2.6) into (2.4) yields the differential equation

$$\left\{\left(\frac{\partial}{\partial t} + \nabla\Phi \cdot \nabla\right)\left(\frac{\partial}{\partial t} + \frac{1}{2}\nabla\Phi \cdot \nabla\right)\Phi + g\frac{\partial \Phi}{\partial y}\right\}_s = 0 \quad . \tag{2.7}$$

To solve Equation (2.7) we expand the velocity potential as follows:

$$\Phi = \Phi^{(o)} + \phi \quad , \tag{2.8}$$

where $\phi$ is the potential associated with the short wavelength surface waves and

$$\Phi^{(o)} \simeq \frac{A_o}{K} \cosh Ky \sin K(x - ct) \quad . \tag{2.9}$$

The separation given by Equation (2.8) essentially couples the short surface waves to the much longer internal waves by superimposing the field potentials.

We substitute the potential from Equation (2.8) into Equation (2.7) and, retaining only up to the linear terms in $\phi$, obtain

$$\left[\frac{\partial^2\phi}{\partial t^2} + \frac{\partial}{\partial t}(\nabla\phi^o\cdot\nabla)\phi + \frac{\partial}{\partial t}(\nabla\phi\cdot\nabla)\phi^o + \nabla\phi^o\cdot\nabla\frac{\partial\phi}{\partial t} + (\nabla\phi^o\cdot\nabla)(\nabla\phi^o\cdot\nabla)\phi\right.$$

$$+ \nabla\phi^o\cdot\nabla(\nabla\phi\cdot\nabla)\phi^o + \nabla\phi\cdot\nabla\frac{\partial\phi^o}{\partial t}$$

$$\left. + \nabla\phi\cdot\nabla(\nabla\phi^o\cdot\nabla)\phi^o\right]_{surface} + \left(g\frac{\partial\phi}{\partial y}\right)_{surface} \simeq 0 \quad . \tag{2.10}$$

This expression may be immediately reduced by using the condition $A_o << c$ and noting that the wavenumber k for the surface wave is very much greater than the wavenumber K for the internal waves, i.e., $K << k$. With these two conditions, Equation (2.10) becomes

$$\left[\frac{\partial^2\phi}{\partial t^2} + g\frac{\partial\phi}{\partial y} + 2\nabla\phi^{(o)}\cdot\nabla\frac{\partial\phi}{\partial t}\right]_{surface} = 0 \tag{2.11}$$

which, together with the Laplacian

$$\nabla^2\phi = \frac{\partial^2\phi}{\partial x^2} + \frac{\partial\phi}{\partial y^2} = 0 \tag{2.12}$$

defines the surface wave potential for our problem. Note that we have assumed the wave to be uniform in the z-direction.

Let us carry out the remaining analysis in terms of an arbitrary traveling internal wave packet $\nabla\phi^o = \vec{U}(x - ct)$. For internal waves whose wavelength is long compared to the depth of the interface along which they propagate, the waves are non-dispersive and arbitrary functions $\vec{U}(\xi)$, $[\xi = x - ct]$, may be considered. This function is analogous to the potential produced by a massive particle from which much lighter particles (surface

waves) are being scattered. Reference to this picture will make the concepts introduced in the following analysis more transparent.

Ball (1964) showed that, for a two-fluid model of the ocean, resonant interactions involving two surface waves and one internal wave can occur. His argument was basically that non-linear quadratic terms in the wave equation can cause a combination wave (frequency $\omega_2$, wavenumber $k_2$) to be generated by the beating of two simple harmonic waves:

$$\omega_2 = \omega_1 \pm \omega$$

and

$$k_2 = k_1 \pm K \qquad (2.13)$$

If this combination [Equation (2.13)] wave matches one of the natural modes of the unperturbed ocean, then a resonance condition exists.

To follow this argument, we consider the wave equation valid for low speed, low amplitude flow [Equation (2.11)], which we can write* as

$$\frac{\partial^2 \phi}{\partial t^2} + g \frac{\partial \phi}{\partial y} = - 2U(x,t) \frac{\partial^2 \phi}{\partial x \partial t} \quad . \qquad (2.14)$$

When the right hand side of Equation (2.14) is approximated by the unperturbed surface wave solution (the Born Approximation)

$$\phi_o \simeq a \cos (k_1 x - \omega_1 t) \qquad (2.15)$$

---

* $U(x,t)$ is assumed to vary slowly over distances and times in which $\phi$ oscillates. Thus, time and space gradients of $U(x,t)$ are neglected.

and the travelling current field by

$$U(x,t) \simeq A \cos(Kx - \omega t) \tag{2.16}$$

[where we have used Equation (2.9)], combination waves are generated. We may use Equations (2.15) and (2.16) in Equation (2.14) to obtain

$$\frac{\partial^2 \phi}{\partial t^2} + g \frac{\partial \phi}{\partial y} = Aa\, k_1 \omega_1 \left\{ \cos\left[(k_1 + K)x - (\omega_1 + \omega)t\right] + \cos\left[(k_1 - K)x - (\omega_1 - \omega)t\right] \right\} \tag{2.17}$$

where $\omega = Kc$.

Of particular interest is the long wavelength, slowly varying difference frequency term. Two waves having almost the same frequency and wavenumber and travelling in the same direction will beat and give rise to an envelope that has a much lower frequency and wavenumber. Any nonlinear terms will result in a generation of a wave component at the beat frequency. The wavenumber of the beat envelope is proportional to the difference between the wavenumbers of the two primary waves. The phase velocity of the beat wave is proportional to the difference between the frequencies of the primary waves and can be shown to be equal to the harmonic mean of the group velocities of the primaries.

When this beat wave matches the internal wave in frequency, wavenumber, and phase velocity, a resonance occurs (see below). In general, the coupling results from various non-linear terms. Quadratic terms involving two surface waves can create combination or beat waves which can resonate with the internal wave. As just discussed above, quadratic terms involving one surface wave and internal wave can cause coupling to a second surface wave.

Hartle and Zachariason (1969) gave a detailed analysis of this problem; that is the solution of Equation (2.14) in the Born Approximation, for waves travelling in the same direction. The right hand side of Equation (2.14) was evaluated with $\phi_o$ taken as the unperturbed surface wave potential and the general problem of an arbitrary travelling current wave was treated. They also gave detailed attention to the variation of wave height and wave slope resulting from the interactions.

The basic features of their solution can be exemplified by treating the special case of a sinusoidal surface current, Equation (2.17). Since we are only concerned with the near resonant case, we consider only the difference frequency term, replace the cosine by an exponential, and find a solution to the equation

$$\frac{\partial^2\phi}{\partial t^2} + g\frac{\partial\phi}{\partial y} = aAk_1\omega_1 \exp\left[i\left\{(k_1-K)x - (\omega_1-Kc)t\right\}\right] . \tag{2.18}$$

We may write $\phi(x,y,t)$ in the form

$$\phi(x,y,t) = \sum_k B(k) \exp\left\{ky - i\left[kx - \omega t\right]\right\} \tag{2.19}$$

so that $\phi \to 0$ as $y \to -\infty$, and we note that for a right travelling wave,

$$\frac{\partial\phi}{\partial y} = -i\frac{\partial\phi}{\partial x} . \tag{2.20}$$

The solution of equ. (2.18) then takes the form, in general,

$$\phi = \sum_j \int \alpha_j \frac{\delta(\omega - \omega_j)\delta(k - k_j)}{\omega^2 - gk} \, d\omega \, dk , \tag{2.21}$$

where $\omega_j$ and $k_j$ are the frequencies and wavenumbers of the combination waves generated by the non-linear terms, i.e., $k_1$-K, and $\omega_1$-Kc for equ.(2.18), and the $\alpha_j$ are the appropriate coefficients. Resonance occurs when, for some j,

$$\omega_j^2 = g k_j \quad . \tag{2.22}$$

In our example, resonance occurs if

$$(\omega_1 - Kc)^2 = g(k_1 - K) \quad . \tag{2.23}$$

Using the fact that $\omega_1^2 = gk_1$, we may reduce Eq. (2.23) to the form

$$2\frac{\omega_1 c}{g} - 1 = \frac{Kc^2}{g} \quad . \tag{2.24}$$

In terms of the surface wave group velocity $c_{g_1}$ ($= g/2\omega_1$), we may write

$$\frac{c}{c_{g_1}} = 1 + \frac{K}{4k_1}\left(\frac{c}{c_{g_1}}\right)^2 \tag{2.25}$$

or, for $K/k_1 << 1$,

$$\frac{c}{c_{g_1}} \simeq 1 \; . \tag{2.26}$$

Thus, resonance obtains when the group velocity of the surface waves is approximately equal to the internal wave velocity. Note that this statement is identical to the statement that the difference wave between two similar surface waves (which could be generated by non-linear effects) match the internal wave in frequency, wavenumber (and phase velocity).

These concepts are more clearly illustrated by reference to the $(k,\omega)$ plane. A point $\vec{\Omega} = (k,\omega)$ in this plane represents a general wave. The curve which is the locus of freely-propagating waves is the dispersion relation $\omega = f(k)$. In general, quadratic non-linear terms will generate sum and difference waves. In particular, a free propagating wave defined by the vector $\vec{\Omega}_2[ = (k_2\omega_2)]$ can couple with an internal wave $\vec{\Omega}[ = (K,\Omega)]$ to produce the beat wave

$$\vec{\Omega}_1 = \vec{\Omega}_2 + \vec{\Omega} \quad .$$

This coupling will be resonant if $\vec{\Omega}_1$ is a characteristic mode of the surface.

Three such combinations are shown in Figure 2c. For two of these the combination wave $(\vec{\Omega}_1)$ does not fall on the locus of freely-propagating waves. However, one such combination does satisfy the resonance condition. It is obvious from the geometry of Figure 2c that, when the internal wave has low frequency ($\Omega << \Omega_2$, $K << k_2$), the slope $\Omega/K$ (which is the internal wave phase velocity c) is essentially equal to the slope of the dispersion curve for waves satisfying the resonance condition, i.e.,

$$c = \frac{\Omega}{K} \sim \frac{d\omega}{dk} = c_g \quad .$$

To examine the resonant and near resonant case it is appropriate to treat an initial value problem where we assume the interaction to be "turned on" at a certain time. For the interaction starting at time $t = 0$, i.e., $\phi'(x,0) = \frac{\partial \phi'}{\partial t}(x,0) = 0$, the solution has the form, [where $\phi = \phi' + a \exp(ik_1 x - i\omega_1 t)$],

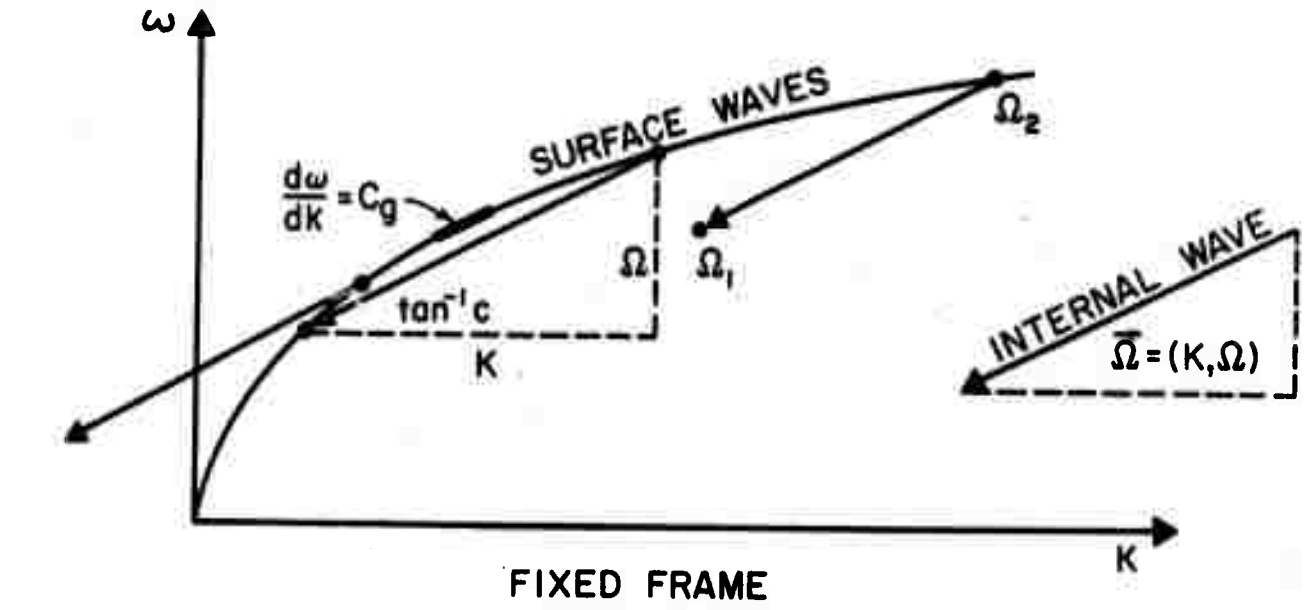


FIXED FRAME

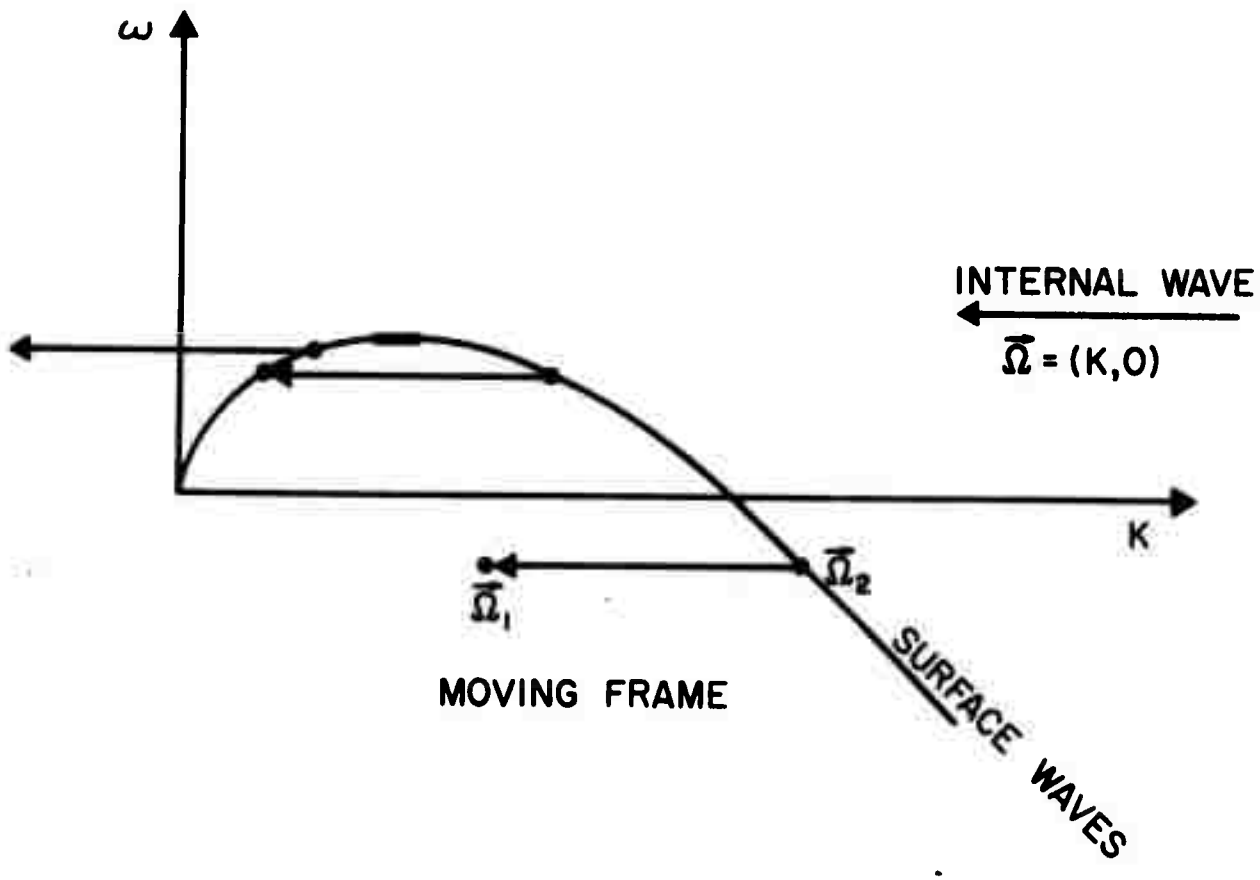


MOVING FRAME

FIGURE 2C. SURFACE WAVE-INTERNAL WAVE INTERACTIONS

$$\phi' = i \frac{A k_1 \omega_1 a}{\omega^*(\omega^* + \omega)} \left\{ \sin \omega^* t - \frac{i\omega^*}{\omega^* - \omega} \left[ 1 - e^{i(\omega^* - \omega)t} \right] e^{-i\omega^* t} \right\} e^{i(k_1 - K)x} \qquad (2.27)$$

where $\omega$ is the difference between the surface wave frequency and the internal wave frequency ($\omega = \omega_1 - Kc$) and $\omega^*$ is the frequency of a surface wave having a wavenumber equal to the difference between that of the surface wave and of the internal wave $\left[\omega^* = \sqrt{g(k_1 - K)}\right]$.

When the exciting frequency $\omega$ is made equal to the frequency $\omega^*$, expand Equation (2.27) and we find that the wave amplitude resonates and grows linearly in time:

$$\phi'(\omega = \omega^*) = i \frac{k_1 \omega_1 Aa}{2\omega^{*2}} \left\{ \sin(\omega^* t) - \omega^* t \, e^{-i\omega^* t} \right\} e^{i(k_1 - K)x} . \qquad (2.28)$$

Close to but not at resonance, the root mean square value of the wave potential is

$$\sqrt{\overline{|\phi|^2}} \simeq \frac{k_1 \omega_1 Aa}{2\omega^*(\omega^* + \omega)} \frac{\omega^*}{|\omega^* - \omega|} . \qquad (2.29)$$

Hartle and Zachariason suggest that the linear growth at resonance will be terminated by either dissipative effects or decay of the internal wave. However, analysis in the following sections indicate that wave reflections may also determine the effective interaction time.

The mathematical reason for the linear growth at resonance in equ. (2.28) arises basically from the introduction of the Born approximation in the calculation of the right hand side of equ. (2.14), where the non-linear terms were replaced by products of the unperturbed surface and internal waves, i.e.,

$\Phi^{(o)}\,\hat{\tau}_o$. As the interaction proceeds the surface wave may be altered, resulting in failure of the Born approximation. It is argued later in this paper that this is indeed what does occur and that the basic process is one of "collision" or scattering (elastic or inelastic) of a surface wave from the surface current pattern. For most of the strongly interacting "collisions" the effective interaction time is determined by the kinematics of this collision or scattering process. In order to treat the near resonance waves it is necessary to proceed beyond the Born approximation and follow the alteration of the surface wave as it interacts with the current pattern. This is done in the following section.

## 3. WAVESCATTER AND REFLECTION

We start, as did Rosenbluth (1971) and Longuet-Higgins/Stewart (1960), from Equations (2.11) and (2.12); that is, linear equations keeping first order interaction terms involving a prespecified, non-uniform, steady surface current. Rosenbluth obtains full wave solutions for a surface wave moving in a region of steady sinusoidal varying current and shows that surface waves can be trapped over the troughs of the internal waves. The solutions exhibit close similarity to those of a quantum mechanical harmonic oscillator and there is an analogy between surface waves trapped in regions of minimum surface current and quantum mechanical particles trapped in regions of minimum potential energy. We will treat the problem of the impingement and reflection of a free surface wave from a region of linearly increasing surface current and show that, for a certain range of wavelengths, the surface waves will be reflected by a travelling current pattern.

### 3A. Dispersion Relations for a steady surface current

Consider a finite region of surface current translating with uniform velocity and described by a function $U(x-ct)$. We transform to a coordinate system moving with this pattern ($\xi = x - ct$) and thus obtain

$$\frac{\partial}{\partial t} \rightarrow \frac{\partial}{\partial t} - c\frac{\partial}{\partial \xi} \quad ; \quad \frac{\partial}{\partial x} \rightarrow \frac{\partial}{\partial \xi} \tag{3.1}$$

so that in this new coordinate system the surface waves in Equation (2.11) obey the equations

$$\left[\phi_{tt} - 2c\phi_{\xi t} + c^2\phi_{\xi\xi} + 2U(\xi)\left\{\phi_{\xi t} - c\phi_{\xi\xi}\right\} + g\phi_y\right]_{\text{surface}} = 0 \tag{3.2}$$

and

$$\phi_{\xi\xi} + \phi_{yy} = 0 \,. \tag{3.3}$$

Taking y to be positive upwards, we may write the general solution of Eq.(3.2) as a superposition of two waves [for surface wavelengths << depth of fluid (D)]

$$\phi = \phi^{(R)} + \phi^{(L)} \tag{3.4}$$

where

$$\phi^{(R)} = \int e^{ky}\, a_k^R(t)\, e^{ikx}\, dk \tag{3.5a}$$

and

$$\phi^{(L)} = \int e^{ky}\, a_k^L(t)\, e^{-ikx}\, dk \quad , \tag{3.5b}$$

which are similar in structure to equ. (2.19). The quantities $\phi^{(R)}$ represent waves traveling to the right and $\phi^{(L)}$ waves to the left in this moving coordinate system. According to Eq. (3.5), we may write

$$\phi_y^{(R)} = -i\phi_x^{(R)} \tag{3.6}$$

and

$$\phi_y^{(L)} = i\phi_x^{(L)} \quad . \tag{3.7}$$

It is to be noted that "traveling to the right" and "traveling to the left" refers to the phase velocity of the surface wave. It was pointed out in section 2 that for this surface-internal wave problem, the most interesting phenomena occur when the group velocity of the surface wave is closely matched to the phase velocity of the internal wave equ. (2.26). Since the surface waves are dispersive, it is possible (and this will be the condition of most interest to us) to have a situation where the phase velocities are in the same, but the group velocities are in opposite, directions for two coupled waves. It occurs that for a given frequency there are four coupled waves that appear in this moving coordinate system. Two of these waves will be shown to have phase velocities to the right, in the direction of the internal wave (R waves), and two have phase

velocities in the opposite direction (L waves). For the two R waves, one turns out to have a group velocity to the right (which we refer to as a (+) wave: $[\phi^{(+R)}]$, and the other has a negative group velocity [a (-) wave: $\phi^{(-R)}$]. The two L waves will similarly be noted as (+) and (-) waves although for these the group velocities have the same sign.

To demonstrate the nature of these waves, we consider an internal wave packet of finite size such as the one shown in Fig. 3a. A packet of surface gravity waves propagating slightly slower (group velocity) than the internal wave will be overtaken and, in the frame moving with the internal wave, these wave packets appear to impinge from the right, whereas faster surface waves impinge from the left. We shall examine the wave field for a single monochromatic surface wave incident on the surface current region (the internal wave packet) from the left [see Fig. 3b] i.e., one moving faster in the moving frame of reference than the internal wave. Since in the moving frame the surface current field is steady, the time dependence of the surface wave potential is of the form $e^{-i\omega t}$ and Eq. (3.2) becomes

$$-\omega^2\phi + i2c\omega\phi_\xi + c^2\phi_{\xi\xi} + 2U(\xi)\left[-i\omega\phi_\xi - c\phi_{\xi\xi}\right] + g\phi_y = 0 \ . \qquad (3.8)$$

This oscillatory time dependence occurs in the coefficient $a_k^L(t)$ and $a_k^R(t)$ in Eqs. (3.5a) and (3.5b).

Before treating the case of a space variable surface current, we examine the dispersion relation when the current is uniform, i.e., $U(\xi) = U_o$ [constant]. To study this case we will reduce Eq. (3.8) to dimensionless form by introducing a characteristic wave number (k*) and frequency ($\omega^*$), i.e., the values for a surface wave traveling at the same velocity (phase) as the internal wave; so that

$$\eta = \omega/\omega^* \quad ; \ \kappa = k/k^* \quad ; \quad \beta = U_o/c \qquad (3.9)$$

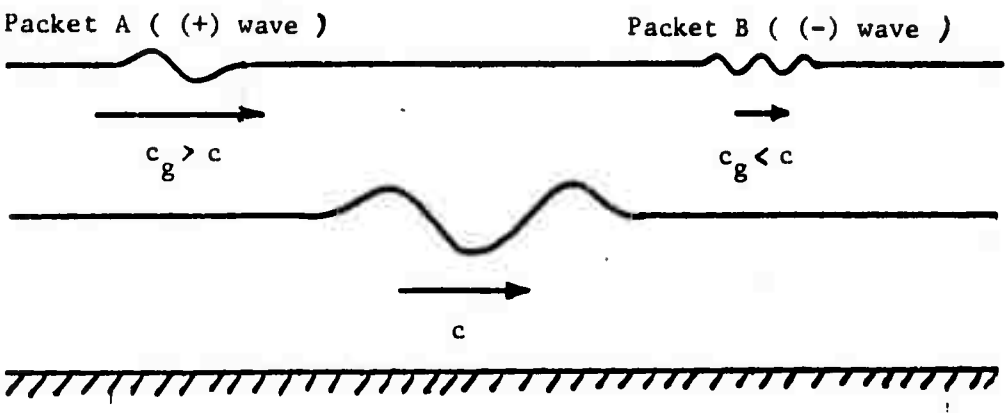


FIGURE 3A. WAVE KINEMATICS BEFORE INTERACTION

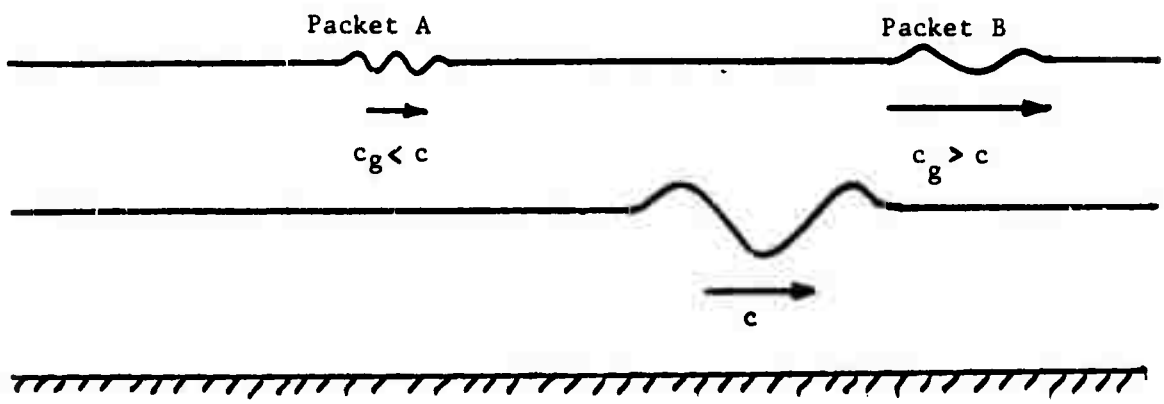


FIGURE 3B. WAVE KINEMATICS AFTER INTERACTION

where $\omega^* = g/c$ and $k^* = g/c^2$. Using the relation $(\partial/\partial\xi \rightarrow ik)$ from Equations (3.1) and (3.6) we can write the dispersion relations for Equation (3.8) as

$$-\eta^2 - 2\eta\kappa - \kappa^2 + 2\beta\left|\eta + \kappa\right|\kappa + \kappa = 0 \quad \text{for the (R) waves} \qquad (3.10a)$$

and

$$-\eta^2 + 2\eta\kappa - \kappa^2 + 2\beta\left|-\eta + \kappa\right|\kappa + \kappa = 0 \quad \text{for the (L) waves} \qquad (3.10b)$$

thereby giving the four waves discussed earlier. We need only follow the formalism for the (R) waves since, according to Equation (3.10)

$$\phi^{(L)}(\eta) = \phi^{(R)}(-\eta)$$

and for these waves

$$\kappa^{\pm} = \frac{1 - 2\eta(1-\beta) \mp \sqrt{1 - 4\eta(1-\beta) + 4\eta^2\beta^2}}{2(1-2\beta)} \quad ; \quad \eta > 0 \ . \qquad (3.11a)$$

To terms linear in $\beta$ this expression agrees with the one obtained more intuitively by replacing the frequency $\omega$ in the dispersion relation calculated in the ocean frame ($\omega = \pm\sqrt{gk}$) by the value expected if the waves are being convected at a velocity $(u-c)$, i.e., $\omega \rightarrow \omega + (c-u)k$. In this case the dispersion relation would become

$$\omega + (c-u)k = \pm\sqrt{gk}$$

or

$$\eta + (1-\beta)\kappa = \pm\sqrt{\kappa} \ .$$

Solving for $\kappa$ yields

$$\kappa = \frac{1 - 2\eta(1-\beta) \pm \sqrt{1 - 4\eta(1-\beta)}}{2(1-\beta)^2} \qquad (3.11b)$$

which agrees with Equation (3.11a) to terms linear in $\beta$. Since the present analysis applies only for values of $\beta$ small compared to unity, we will use (3.11a) or (3.11b) interchangeably.

In Figure 4 we have plotted the dispersion relation in terms of the reduced variables $\eta$ and $\kappa$. We are patricularly interested in regions near the turning point where the group velocity vanishes and the surface wave packet travels with a velocity near that of the internal wave phase. In this region the two R waves are strongly coupled. However, as is discussed later, the coupling to the L waves is weak and we ignore it entirely here. Thus, we delete the L,R superscripts and refer hereafter only to (+) and (-) waves, (both of which will always be R waves).

We now return to the problem of a finite region of surface current. We are treating the case of an overtaking packet incident on this region from the left. This wave [a (+) wave], in general, will be partially transmitted [as a (+) wave] by the current region and partially reflected [as a (-) wave].* If we define r as the coefficient of the reflected wave and t as the coefficient of the transmitted wave, then we may write the potential far to the left of this interaction region as

$$\phi = \phi_o \left\{ e^{i\left[k_\infty^{(+)}\xi - \omega t\right]} + r\, e^{i\left[k_\infty^{(-)}\xi - \omega t\right]} \right\} \qquad (3.12a)$$

* The meaning of reflected and transmitted will become clear later as we develop the concept of the surface wave packet later in this section.

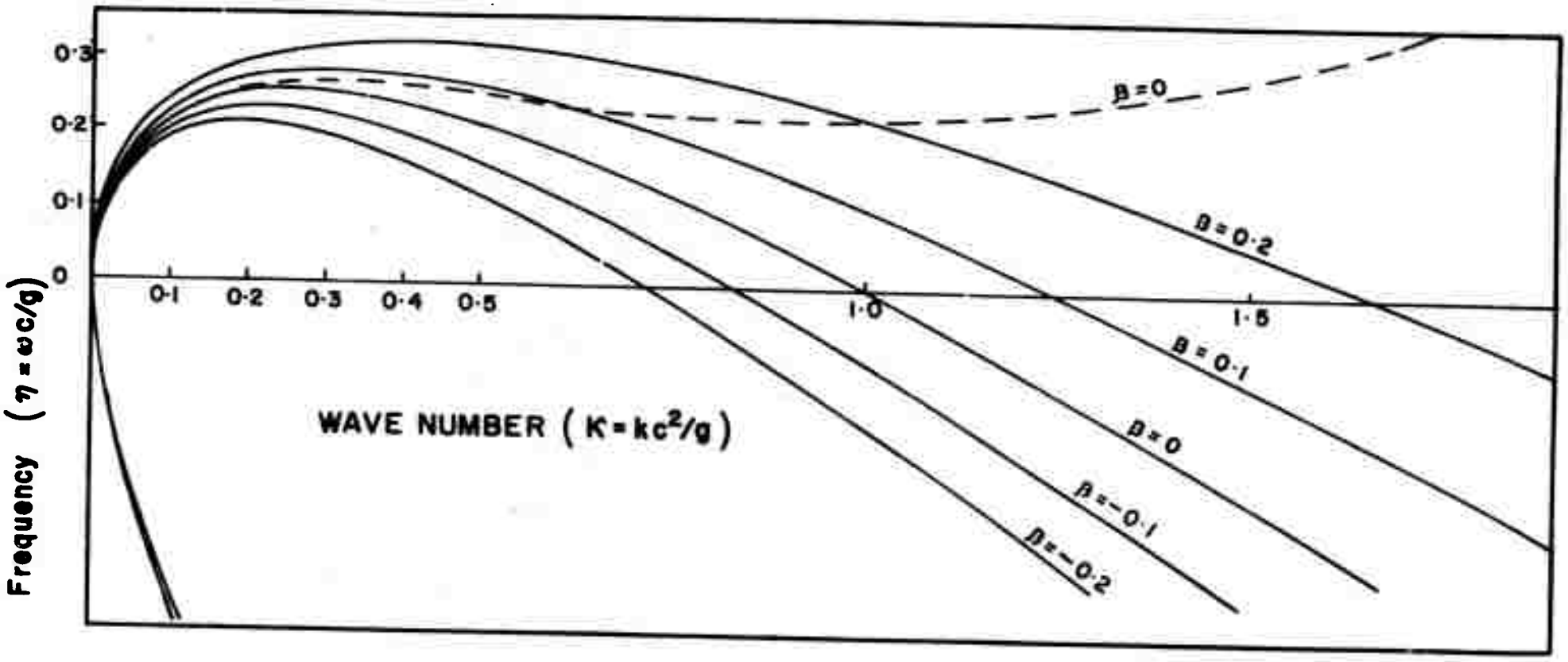


FIGURE 4. THE DISPERSION RELATION FOR GRAVITY WAVES IN A MOVING FRAME.
(THE DASHED LINE INCLUDES SURFACE TENSION EFFECTS.)

where $\phi_o$ is the amplitude of the incident wave. Further, there will be only a transmitted wave far to the right of the region:

$$\phi = \phi_o \, t \, e^{i\left[k_\infty^{(+)}\xi - \omega t\right]} \tag{3.12b}$$

for $\xi \to +\infty$. The wavenumbers $k_\infty^{(+)}$ and $k_\infty^{(-)}$ are defined in the undisturbed region of the surface, i.e., where $\beta = 0$. One may therefore use the dispersion relations from Equation (3.10) to obtain for the R waves

$$\kappa_\infty^{\pm} = \frac{1}{2}\left(1 - 2\eta \mp \sqrt{1 - 4\eta}\right) \tag{3.13a}$$

or

$$\kappa_\infty^{\pm} = \frac{g}{2c^2}\left[1 - \frac{2\omega c}{g} \mp \sqrt{1 - \frac{4\omega c}{g}}\right]. \tag{3.13b}$$

If $\omega > g/4c$, therefore, there are no right propagating waves in the frame of the moving internal wave. The distortion or reflection of the surface wave as it travels through the current region depends critically on the variation of the wave number $\kappa^{(\pm)}$ with changes in U .

It is useful to attempt to interpret the concepts of Ball and of Longuet-Higgins/Stewart in terms of the scattering or reflection mechanism. In the reference frame moving with the internal wave the strongly interacting (reflecting) free waves form a standing wave pattern on one side of the reflection point (see Fig. 5). This standing wave consists of two wave trains having (in this frame) equal but opposite group velocities but phase velocities in the same direction. Although the mean group velocity is zero (so that the standing wave pattern does not move) the mean phase velocity is non-zero. Individual wavelets (or points of constant phase) appear to move through the standing wave pattern. For example, for a left incident wave, a wavelet will appear to be

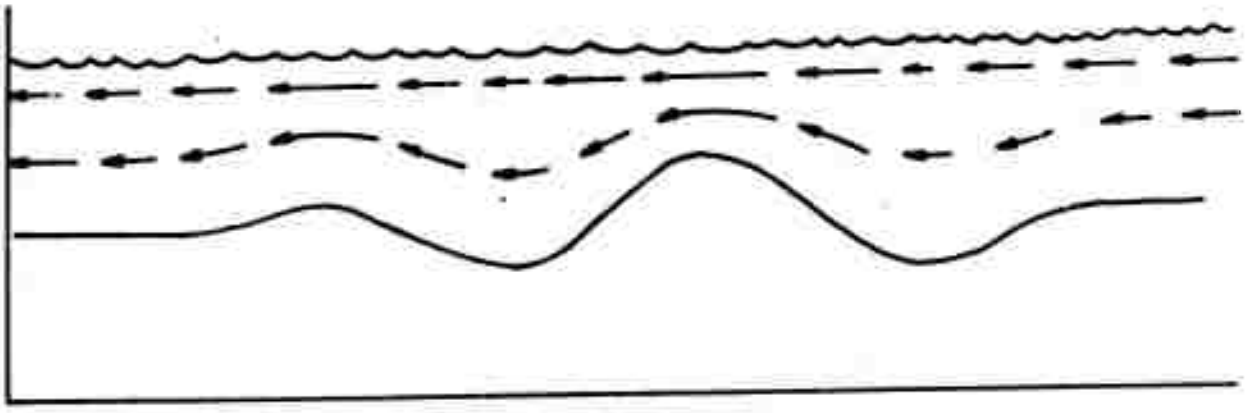

FIGURE 5A. CURRENTS ABOVE THE INTERNAL WAVE

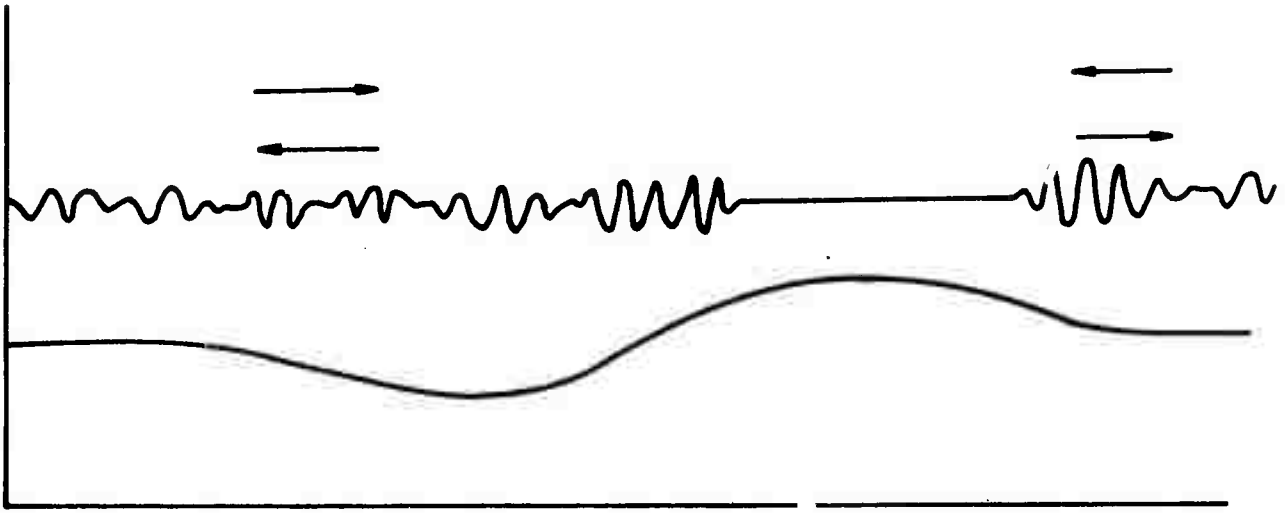

FIGURE 5B. UNTRAPPED WAVE REFLECTING FROM THE CREST REGION OF THE INTERNAL WAVE

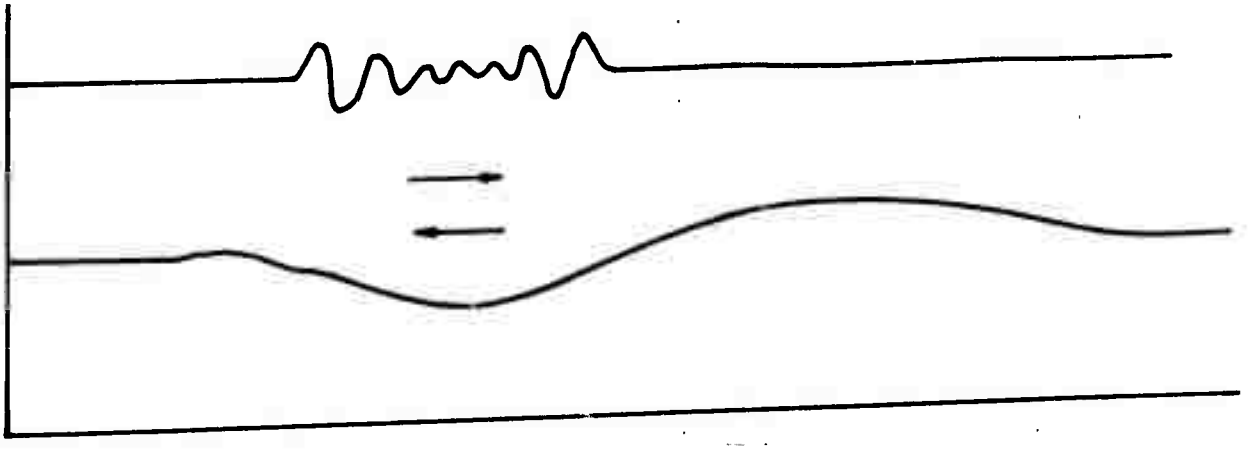

FIGURE 5C. WAVES TRAPPED IN THE TROUGH OF AN INTERNAL WAVE

born on the left side of the standing wave region, to travel to the right through the pattern, its amplitude undergoing a quasi-periodic modulation by the standing wave and finally dying or disappearing at the front edge of the standing wave region, i.e., the reflection point. According to the Born approximation of Ball and Hartle/Zachariason, the stationary current pattern induces a secondary wave that, together with the incident wave, creates a stationary standing wave pattern. This induced wave must therefore have a group velocity equal and opposite to the incident wave (since the mean group velocity is equal to the phase velocity of the standing wave, i.e., to zero). Thus, it should be possible to interpret the Born approximation results near resonance in terms of the creation of a scattered wave whose wavenumber and frequency are dependent on the difference between those of the incident wave and that of a perfectly resonant wave (i.e., one for which $c_g = c$).*

### 3B. Scattering at a Boundary

The preceeding section was concerned with the long range effects of the internal current on the surface waves. This section will study the surface waves in the interaction region. To this end, we note that when the internal current increases over a limited region of space two effects contribute to the observables of interest: 1) the variation of the wave slope as it passes through the surface current region, and 2) the generation of reflected waves at regions where the wavenumber changes rapidly.

---

* Although a mechanism allowing for depletion of the incident wave would probably be required to get reasonable results at later times.

In order to solve this latter problem for somewhat arbitrary $U(\xi)$, we modify the formulation of the problem slightly. We divide the surface current region into a number of sections, each having a width small compared to the wavelength of the internal wave [Fig. 6]. We index the positions along the internal wave by $\xi_j$ and let the interval between any two steps j and (j+1) be $\Delta\xi_j$. An incident wave will generate both transmitted and reflected waves as it impinges on each of these steps. Within each section the surface current is taken to be uniform so that the wave potential in the region between $\xi_j$ and $\xi_{j+1}$ has the general form

$$\phi_j = A_j \exp\left[i\left(k_j^{(+)}\xi - \omega t\right)\right] + B_j \exp\left[i\left(k_j^{(-)}\xi - \omega t\right)\right] \tag{3.14}$$

where $k_j^{(+)}$ and $k_j^{(-)}$ are determined from the dispersion relation for the $j^{th}$ slab. The values of $A_j$ and $B_j$ are found by matching boundary conditions at all the interfaces between the individual sections (see Figure 7). The number of independent component waves that need to be allowed for in Equation (3.14) is two in our present case (gravity waves). In general this number is equal to the number of allowable propagating wavenumbers that have the same frequency. In the capillary-gravity regime where surface tension effects are important, it is possible to have these intersections of the dispersion curve for a given frequency $\omega$ (see Figure 4), thus requiring three independent waves in Equation (3.14). We carry out the present formalism for gravity waves only. The generalization to the capillary-gravity regime will be made subsequently.

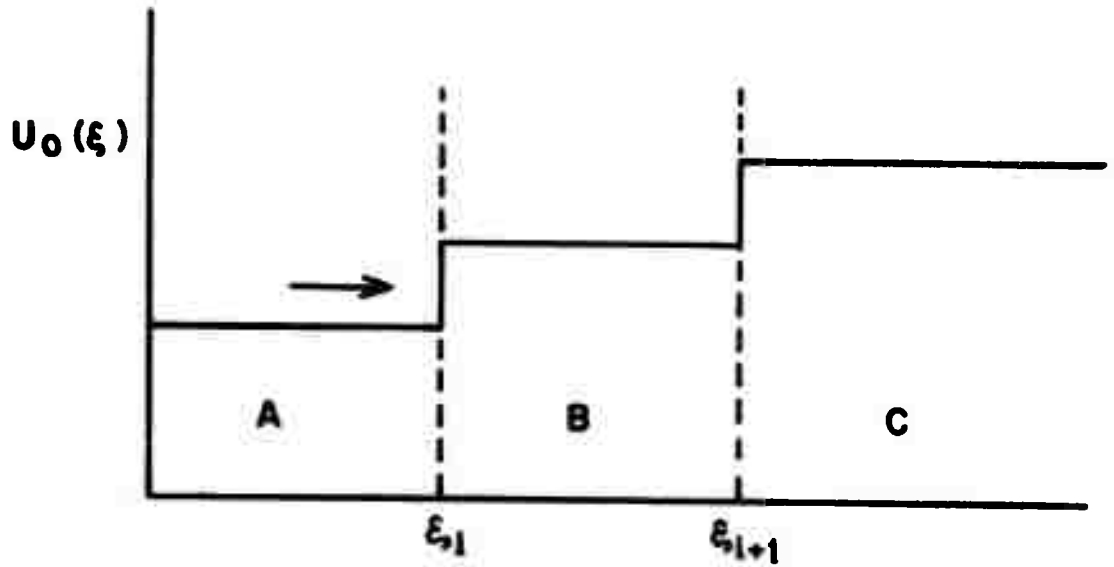


FIGURE 6. FINITE DIFFERENCE APPROXIMATION OF THE SURFACE CURRENT

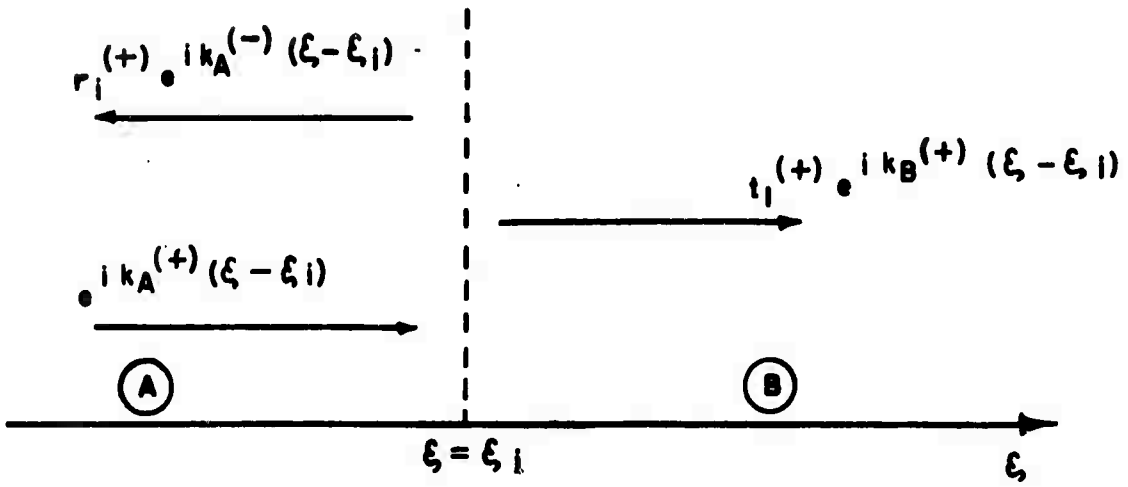


Fig. 7a. LEFT INCIDENT WAVE.

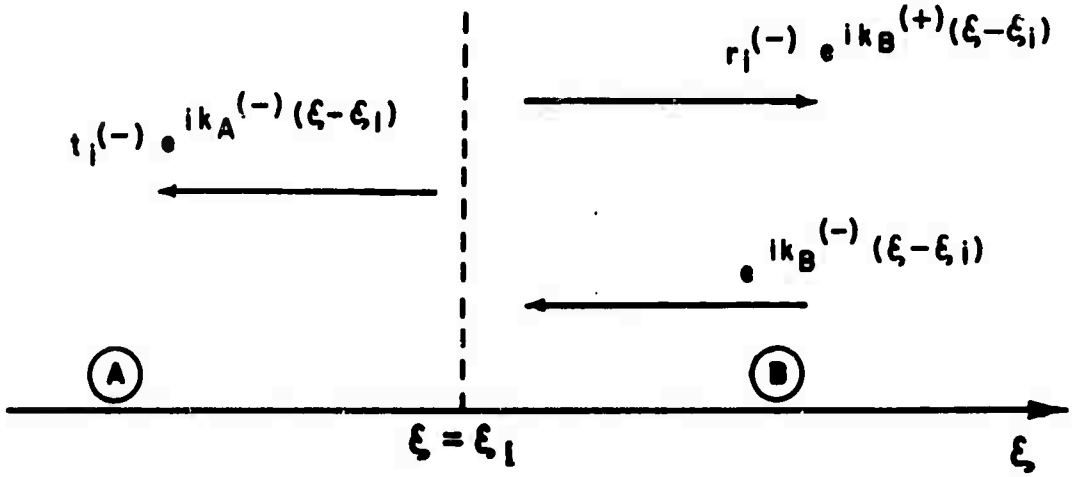


Fig. 7b. RIGHT INCIDENT WAVE.

The two cases to be considered are ahown in Figure 7: an incident wave traveling from left to right (+) of unit amplitude is shown in Figure (7a) while a wave of unit amplitude incident from right (-) is shown in Figure (7b). Note that we are discussing the R-solutions of Equation (3.10a), which has been decomposed into these (+) and (-) waves in the moving coordinate system of the internal wave. Figure 7 is actually a blow-up of the step regions shown in Figure 6. Since we are treating quantities discretely in this section, both the reflection ($r_j$) and transmission ($t_j$) coefficients for the waves carry an index to distinguish the boundary to which they refer, i.e., point in space. An additional index of (+) and (-) is carried by these coefficients as well as the wavenumbers to distinguish the direction (group velocity) of the incident wave with which they are associated.

The continuity of the amplitude and slope of the waves at the $j^{th}$ boundary, between regions A and B in Figure 7 requires that

$$\phi_i(\xi = \xi_j) + \phi_r(\xi = \xi_j) = \phi_t(\xi = \xi_j) \tag{3.15}$$

and

$$\frac{1}{\phi_i}\frac{d\phi_i}{d\xi}\bigg|_{\xi=\xi_j} + \frac{1}{\phi_r}\frac{d\phi_r}{d\xi}\bigg|_{\xi=\xi_j} = \frac{1}{\phi_t}\frac{d\phi_t}{d\xi}\bigg|_{\xi=\xi_j} \tag{3.16}$$

where the subscripts refer to the incident (i), reflected (r) and transmitted (t) waves. For an incident wave traveling from left to right (Figure 7a), we have from Equations (3.15) and (3.16) the continuity conditions that

$$1 + r_j^{(+)} = t_j^{(+)} \tag{3.17}$$

and

$$k_A^{(+)} + r_j^{(+)}\, k_A^{(-)} = t_j^{(+)}\, k_B^{(+)} \quad . \tag{3.18}$$

Similarly, for an incident wave traveling from right to left [Fig. 7b], we obtain

$$1 + r_j^{(-)} = t_j^{(-)} \tag{3.19}$$

and

$$k_B^{(-)} + r_j^{(-)}\, k_B^{(+)} = t_j^{(-)}\, k_A^{(-)} \quad . \tag{3.20}$$

The reflection and transmission amplitudes across the boundary may be evaluated in terms of the wave numbers in the two regions by using Equations (3.17) - (3.20),

$$t_j^{(+)} = \left[k_A^{(+)} - k_A^{(-)}\right] \Big/ \left[k_B^{(+)} - k_A^{(-)}\right] \quad , \tag{3.21a}$$

$$r_j^{(+)} = \left[k_A^{(+)} - k_B^{(+)}\right] \Big/ \left[k_B^{(+)} - k_A^{(-)}\right] \quad , \tag{3.21b}$$

$$t_j^{(-)} = \left[k_B^{(-)} - k_B^{(+)}\right] \Big/ \left[k_A^{(-)} - k_B^{(+)}\right] \quad , \tag{3.22a}$$

and

$$r_j^{(-)} = \left[k_B^{(-)} - k_A^{(-)}\right] \Big/ \left[k_A^{(-)} - k_B^{(+)}\right] \quad . \tag{3.22b}$$

The value of obtaining these expressions will become evident when we allow the interval between steps to become very small. It will then be possible to represent these differences in wavenumbers in terms of derivatives. This construction is carried out later in this section and is also used in Section 4.

To broaden our problem slightly, let us consider a wave of unit amplitude incident from the left on a current pattern of finite extent [see Figure 8]. We know that the general long distance solution to this problem can be given by the superposition of the incident and reflected wave to the left of the region and a transmitted wave far to the right [see Equations (3.12a) and (3.12b)]. To formalize these statements we define a two vector $\psi$ whose components are the local values of the (+) and (-) waves

$$\psi = \begin{pmatrix} \phi^{(+)} \\ \phi^{(-)} \end{pmatrix}$$

We also define a scattering matrix $S$ with elements $s_{ij}$ which relates the wave vector $(-\infty)$ far to the left of the current region to the vector on the right hand side

$$\psi(+\infty) = S\ \psi(-\infty) \quad .$$

In order to evaluate the elements of $S$, we consider two hypothetical scattering experiments. Suppose first a (+) wave of unit amplitude is incident on the region from the left (Figure 8). The amplitude of the transmitted wave is $T^{(+)}$ and that of the reflected wave [which is a (-) wave] is defined as $R^{(+)}$. Then we must have

$$\begin{bmatrix} T^{(+)} \\ 0 \end{bmatrix} = \begin{bmatrix} s_{11} & s_{12} \\ s_{21} & s_{22} \end{bmatrix} \begin{bmatrix} 1 \\ R^{(+)} \end{bmatrix} \tag{3.23}$$

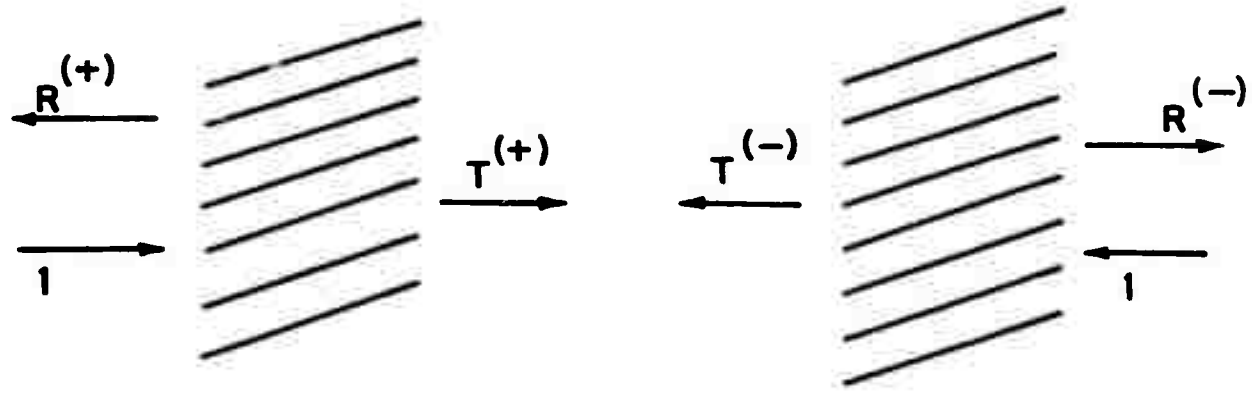


Figure 8. Reflection and transmission coefficients for the entire current region.

or

$$R^{(+)} = -s_{21}/s_{22} \tag{3.24a}$$

and

$$T^{(+)} = s_{11} - s_{12}\, s_{21}/s_{22} \,. \tag{3.24b}$$

In a similar manner, for a wave of unit amplitude incident from the right (Figure 8) with reflected and transmitted amplitudes $R^{(-)}$ and $T^{(-)}$, respectively, we may write.

$$\begin{bmatrix} R^{(-)} \\ 1 \end{bmatrix} = \begin{bmatrix} s_{11} & s_{12} \\ s_{21} & s_{22} \end{bmatrix} \begin{bmatrix} 0 \\ T^{(-)} \end{bmatrix} \tag{3.25}$$

or

$$R^{(-)} = s_{12}/s_{22} \tag{3.26a}$$

and

$$T^{(-)} = 1/s_{22} \,. \tag{3.26b}$$

The matrix S is the scattering matrix for the entire current region. The reflection amplitudes $R^{(+)}$ and $R^{(-)}$, as well as the transmitted wave amplitudes $T^{(+)}$ and $T^{(-)}$ also refer the entire surface current region. We may use Equations (3.24) and (3.26) to express the elements of the scattering matrix in terms of these "measured" reflection and transmission coefficients:

$$s_{22} = 1/T^{(-)} \,, \tag{3.27a}$$

$$s_{12} = R^{(-)}/T^{(-)} \,, \tag{3.27b}$$

$$s_{21} = -R^{(+)}/T^{(-)} \,, \tag{3.27c}$$

and

$$s_{11} = T^{(+)} - R^{(-)}\, R^{(+)}/T^{(-)} \,. \tag{3.27d}$$

These elements may now be applied to the analysis of the characteristic of the $j^{th}$ boundary which initiated this subsection.

We define a two-component vector $\psi_j$ made up of the amplitudes of the right $[\phi_j^{(+)}]$ and left $[\phi_j^{(-)}]$ travelling waves at a point just to the right of the $j^{th}$ interface:

$$\psi_j = \begin{bmatrix} \phi_j^{(+)} \\ \phi_j^{(-)} \end{bmatrix} . \tag{3.28}$$

Using a propagation matrix $P_j$ and a reflection or scattering matrix $S_j$, we may write the vector at the $(j+1)^{th}$ step in terms of its value at the $j^{th}$ step, by

$$\psi_{j+1} = P_j \cdot S_j \cdot \psi_j \tag{3.29}$$

where the waves incident on the $j^{th}$ boundary are scattered by the matrix $S_j$ and propagated across the uniform interval from $\xi_j$ to $\xi_{j+1}$ by the propagation matrix $P_j$. If the entire current region has been divided into N steps, then the wave amplitude $\psi_{N+1}$ to the right of this region is related to the amplitude $\psi_1$ to the left of the region, according to

$$\psi_{N+1} = \left\{ \prod_{j=1}^{N} S_j \cdot P_j \right\} \psi_1 \tag{3.30}$$

or

$$\psi_{N+1} = S \psi_1 , \tag{3.31}$$

where S is now the scattering matrix for the entire region:

$$S = \prod_{j=1}^{N} P_i \cdot S_j . \tag{3.32}$$

Thus the matrix S introduced in Equation (3.11) for a wave crossing an arbitrary region can be thought of as being constructed from a sequence of weak scatterings.

A little thought will convince one that the reflection (scattering) matrix $S_j$ at each of the steps $\xi_j$ has the same structure as the scattering matrix S for the entire region. We may therefore, write the matrix $S_j$ in terms of the reflection and transmission coefficients $r_j$ and $t_j$ as follows:

$$S_j = \begin{bmatrix} t_j^{(+)} - r_j^{(+)} r_j^{(-)} / t_j^{(-)} & r_j^{(-)} / t_j^{(-)} \\ -r_j^{(+)} / t_j^{(-)} & 1/t_j^{(-)} \end{bmatrix} . \qquad (3.33)$$

The propagation matrix $P_j$ carries the translation information for the process and may be written as

$$P_j = \begin{bmatrix} \exp\left\{ik^{(+)}[\xi_{j+1}-\xi_j]\right\} & 0 \\ 0 & \exp\left\{ik^{(-)}[\xi_{j+1}-\xi_j]\right\} \end{bmatrix} . \qquad (3.34)$$

If we assume that the reflections described by Equation (3.31) are weak, then it is possible to write the reflection matrix above [Equation (3.33)] in an approximate form. For weakly reflected waves we can neglect all terms in $S_j$ which are second order in the reflection coefficients, $r_j^{(+)}$ and $r_j^{(-)}$. Also, we may expand the inverse of the (-) transmission coefficient as,

$$\frac{1}{t_j^{(-)}} = \frac{1}{1+r_j^{(-)}} \approx 1 - r_j^{(-)} + \ldots \qquad (3.35)$$

Using Equation (3.35) and neglecting terms quadratic in the reflection coefficients, we write the scattering matrix as,

$$S_j \approx 1 + R_j \tag{3.36}$$

where

$$R_j = \begin{bmatrix} r_j^{(+)} & r_j^{(-)} \\ -r_j^{(+)} & -r_j^{(-)} \end{bmatrix} \tag{3.37}$$

where $R_j^2$ is considered negligible in this approximation. This implies that there is only a single scattering from each of the steps and that the reflected surface wave is a linear superposition of each of these small reflections.

Let us consider the generation of these reflected waves by Equation (3.32). If we impose our weak reflection condition, Equation (3.36), then all terms of order $R_j^2$ and higher in this product may be neglected. A general term which would contribute to the scattering matrix would, therefore, be linear in $R_j$, i.e., be of the form

$$P_N P_{N-1} \cdots P_j R_j P_{j-1} \cdots P_2 P_1 \ . \tag{3.38}$$

Physically, Equation (3.38) means that the incident wave will propagate freely through the first j-1 steps of the steady current region; at the $j^{th}$ step it will interact weakly with the internal wave, as specified by the matrix $R_j$, and then continue to propagate without further interaction.

One can easily show that the product of propagation matrices preceding the interacting in Equation (3.38) can be written in the continuous limit as,

$$P_{j-1}\,P_{j-2}\cdots P_2\,P_1 = \begin{bmatrix} \exp\left\{i\int_{\xi_1}^{\xi_{j-1}} k^{(+)}(\xi')d\xi'\right\} & 0 \\ 0 & \exp\left\{i\int_{\xi_1}^{\xi_{j-1}} k^{(-)}(\xi')d\xi'\right\} \end{bmatrix} \tag{3.39}$$

by using the definition of the P's [Equation (3.34)]. It is also clear that in general, the amplitude of the incident wave is being modulated by the internal wave packet.

## 3C. Differential Formulation of the Propagation Equations

In this section we will construct a set of differential equations to govern the variations of the forward and backward propagating waves [$\phi^{(+)}$ and $\phi^{(-)}$] by taking the limit of very small $\xi$ intervals in the propagation equations [Equations (3.21) to (3.22)]. In the limit of small $\xi_{j+1} - \xi_j = \Delta\xi$, the transmission and reflection amplitudes become,

$$r_j^{(+)} = -\frac{\Delta\xi}{\left[\kappa^{(+)} - \kappa^{(-)}\right]}\,\frac{d\kappa^{(-)}}{d\xi} \tag{3.40}$$

$$r_j^{(-)} = -\frac{\Delta\xi}{\left[\kappa^{(+)} - \kappa^{(-)}\right]}\,\frac{d\kappa^{(-)}}{d\xi} \tag{3.41}$$

$$t_j^{(-)} = 1 + r_j^{(-)} \tag{3.42}$$

and

$$t_j^{(+)} = 1 + r_j^{(+)} \quad . \tag{3.43}$$

Equations (3.40) and (3.41) will be derived in Section 4, where a complete discussion of their characteristics will be given.

The dispersion relation [Equation (3.11)] (neglecting quadratic terms in $\beta$) may be written in the form

$$\kappa^{\pm} = \kappa_1 \mp \kappa_2 \tag{3.44}$$

where

$$\kappa_1 = \frac{1 - 2\eta(1-\beta)}{2(1-2\beta)} \tag{3.45a}$$

and

$$\kappa_2 = \frac{\sqrt{1 - 4\eta(1-\beta)}}{2(1-2\beta)} \tag{3.45b}$$

For very small values of the difference $\xi_{j+1} - \xi_j = \Delta\xi_j$ the scattering matrix for weak reflections [Equation (3.36)], using Equations (3.40) to (3.45), can be rewritten as

$$S_j = \begin{bmatrix} 1 & 0 \\ 0 & 1 \end{bmatrix} + \frac{d\kappa_1}{d\xi}\frac{\Delta\xi_j}{2\kappa_2}\begin{bmatrix} 1 & 1 \\ -1 & -1 \end{bmatrix} + \frac{d\kappa_2}{d\xi}\frac{\Delta\xi_j}{2\kappa_2}\begin{bmatrix} -1 & 1 \\ 1 & -1 \end{bmatrix} \tag{3.46}$$

Similarly, the propagation matrix given by Equation (3.34) may be expanded to obtain

$$P_j = \begin{bmatrix} 1 & 0 \\ 0 & 1 \end{bmatrix} + \begin{bmatrix} ik^*(\kappa_1 - \kappa_2)\Delta\xi_j & 0 \\ 0 & ik^*(\kappa_1 + \kappa_2)\Delta\xi_j \end{bmatrix} \tag{3.47}$$

From the recursion relation [Equation (3.29)] we have

$$\Delta\xi_j \frac{d\psi_j}{d\xi} \approx \psi_{j+1} - \psi_j = \left(P_j S_j - 1\right)\psi_j \tag{3.48}$$

where $\psi_j$ is defined as the two component wave given by Equation (3.28). Introducing Equations (3.46) and (3.47) into Equation (3.48) and keeping only

terms which are linear in $\Delta\xi_j$, we obtain the following coupled equations for the wave components $\phi^{(+)}$ and $\phi^{(-)}$:

$$\frac{d\phi^{(+)}}{d\xi} = ik^*(\kappa_1 - \kappa_2)\phi^{(+)} + \frac{1}{2\kappa_2}\frac{d\kappa_1}{d\xi}\left[\phi^{(+)} + \phi^{(-)}\right] - \frac{1}{2\kappa_2}\frac{d\kappa_2}{d\xi}\left[\phi^{(+)} - \phi^{(-)}\right] \quad (3.49)$$

and

$$\frac{d\phi^{(-)}}{d\xi} = ik^*(\kappa_1 - \kappa_2)\phi^{(-)} - \frac{1}{2\kappa_2}\frac{d\kappa_1}{d\xi}\left[\phi^{(+)} + \phi^{(-)}\right] + \frac{1}{2\kappa_2}\frac{d\kappa_2}{d\xi}\left[\phi^{(+)} - \phi^{(-)}\right] \quad (3.50)$$

in the continuous limit. These equations may be simplified if we introduce the sum and difference amplitudes S and D:

$$S = \left[\phi^{(+)} + \phi^{(-)}\right] \exp\left\{-i\int k^* \kappa_1 \, d\xi\right\} \quad (3.51)$$

and

$$D = \left[\phi^{(+)} - \phi^{(-)}\right] \exp\left\{-i\int k^* \kappa_1 \, d\xi\right\} . \quad (3.52)$$

By adding and subtracting Equations (3.49) and (3.50) and using Equations (3.51) and (3.52) we obtain,

$$\frac{dS}{d\xi} = -ik^* \kappa_2 D \quad (3.53)$$

and

$$\frac{dD}{d\xi} = -\frac{1}{\kappa_2}\frac{d\kappa_2}{d\xi} D + \left[\frac{1}{\kappa_2}\frac{d\kappa_1}{d\xi} - ik^* \kappa_2\right] S . \quad (3.54)$$

We may eliminate D from these latter equations with a little algebraic manipulation and obtain

$$\frac{d^2S}{d\xi^2} + \left[(k^*\kappa_2)^2 + ik^* \frac{d\kappa_1}{d\xi}\right] S = 0 \quad (3.55)$$

as the equation for the wave envelope.

## 3D. Solutions in the Neighborhood of a Turning Point

Near $\kappa_2 = 0$ , Equation (3.49) and (3.50) are singular. Near these singular regions (turning points), we may approximate the current pattern by a linear form. Equation (3.55), familiar to those concerned with electromagnetic propagation in a medium having a variable refractive index, has an explicit solution when the current ($= c\beta = -c\varepsilon$) varies linearly with position. To see this, let us define a critical value for the adverse current $\varepsilon_o$ , i.e., $\varepsilon_o = \frac{1}{4\eta} - 1$ , and define

$$\varepsilon = \varepsilon_o(1 + \xi/\Delta) \quad \text{for} \quad -\Delta < \xi < 0 \ . \tag{3.56}$$

Using the definitions of $\kappa_1$ and $\kappa_2$ from Equation (3.45) in conjunction with Equation (3.56), we find that the imaginary term in Equation (3.55) is negligible in comparison to the $(k^*\kappa_2)^2$ term when

$$|\xi| \gg \frac{2}{k^*} = \frac{\lambda^*}{\pi} \ . \tag{3.57}$$

With this condition Equation (3.55) reduces to

$$\frac{d^2S}{d\xi^2} - \left(\frac{k^*}{2}\right)^2 \frac{\varepsilon_o}{\Delta} \xi \, S = 0 \ , \tag{3.58}$$

which is valid when the wave envelope is much more than a characteristic wavelength away from the reflection point.

Equation (3.58) is the equation for the Airy integral in terms of the variable $\zeta$:

$$\zeta = \left(\frac{k^2\varepsilon_o}{4\Delta}\right)^{1/3} \xi \tag{3.59}$$

that is,

$$\frac{d^2S}{d\zeta^2} - \zeta S = 0 \ . \tag{3.60}$$

The form of the solution is that of a varying amplitude standing wave.

The wave amplitudes which are solutions of Equations (3.49) and (3.50) are expressed in terms of the Airy integral [Ai(ζ)] according to

$$\phi^{(+)} = \frac{D + S}{2} \exp\left\{ i \int k^* \kappa_1 \, d\xi \right\} \tag{3.61}$$

$$\phi^{(-)} = \frac{S - D}{2} \exp\left\{ i \int k^* \kappa_1 \, d\xi \right\} \tag{3.62}$$

where

$$S = Ai(\zeta)\, C_1 \tag{3.63}$$

from Equation (3.60), and

$$D = \frac{1}{|\xi|^{1/2}} \frac{dS}{d\xi} \tag{3.64}$$

from Equation (3.53). Here, ζ is expressed in terms of ξ in Equation (3.59) and $C_1$ is a constant. The constant $C_1$ can be determined by examining the asymptotic form of Ai(ζ), which for $\zeta << 0$ is,

$$Ai(\zeta) \sim \frac{1}{\sqrt{\pi}\ |\zeta|^{1/4}} \sin\left( \frac{2}{3} |\zeta|^{3/2} + \frac{\pi}{4} \right) . \tag{3.65}$$

Thus, using Equation (3.63), we obtain for the asymptotic form of the total wave envelope,

$$S = \frac{1}{\sqrt{\pi}\ |\zeta|^{1/4}} \sin\left( \frac{2}{3} |\zeta|^{3/2} + \frac{\pi}{4} \right) . \tag{3.66}$$

Using Equation (3.66) in conjunction with Equation (3.64) we find

$$D = \frac{iC_1}{\sqrt{\pi}} \left\{ \frac{\cos\left( \frac{2}{3} |\zeta|^{3/2} + \frac{\pi}{4} \right)}{|\zeta|^{1/4}} \right\} \tag{3.67}$$

as the asymptotic expression for the wave difference. Normalized to a unit incident amplitude [$\phi^{(+)} = 1$] at $\xi = -\Delta$, the asymptotic form of the incident and reflected waves are

$$\frac{\phi^{(+)}}{\phi_o^{(+)}} = \left(\frac{\Delta}{|\xi|}\right)^{1/4} \exp\left\{ik^*\left[\int \kappa_1\, d\xi - \frac{1}{3}\sqrt{\frac{\epsilon_o}{\Delta}}\,|\xi|^{3/2}\right] - i\,\frac{\pi}{4}\right\} \tag{3.68}$$

and

$$\frac{\phi^{(-)}}{\phi_o^{(-)}} = \left(\frac{\Delta}{|\xi|}\right)^{1/4} \exp\left\{ik^*\left[\int \kappa_1\, d\xi + \frac{1}{3}\sqrt{\frac{\epsilon_o}{\Delta}}\,|\xi|^{3/2}\right] + i\,\frac{\pi}{4}\right\} \tag{3.69}$$

The velocity potential of the total wave has the modulated envelope:

$$\Phi = 2\phi_o\left(\frac{\Delta}{|\xi|}\right)^{1/4} \cos\left\{\frac{k^*}{3}\sqrt{\frac{\epsilon_o}{\Delta}}\,|\xi|^{3/2} - \frac{\pi}{4}\right\} \exp\left\{ik^*\int \kappa_1\, d\xi - i\omega t\right\} \tag{3.70}$$

as does the wave height $y_s$. The wave height may be obtained from the equation

$$y_s = \int \frac{dy_s}{dt}\, dt = \int \phi_y\, dt$$

which using Equations (3.5) and (3.6) yields

$$y_s = \frac{1}{\omega}\left(\frac{\partial \phi}{\partial x}\right)_s \quad . \tag{3.71}$$

For an incident wave whose peak amplitude at $\xi = -\Delta$ is $\Delta Y$, the wave height as a function of position is the real part of

$$k^*\left(\frac{\Delta}{|\xi|}\right)^{1/4} \frac{\Delta Y}{\omega}\left\{\frac{i}{2}\, k^*\kappa_1 \cos z - \sqrt{\frac{\epsilon_o}{\Delta}}\,|\xi|^{1/2} \sin z\right\} \exp\left\{ik^*\int \kappa_1\, d\xi - i\omega t\right\}$$

where

$$z = \frac{k^*}{3}\sqrt{\frac{\epsilon_o}{\Delta}}\,|\xi|^{3/2} - \frac{\pi}{4}$$

or in other words

$$y_s(\xi) = \frac{2k^*}{\omega}\left(\frac{\Delta}{|\xi|}\right)^{1/4}\left[\kappa_1 \cos(z-\pi) \sin\left\{k^*\int \kappa_1\, d\xi - \omega t\right\}\right.$$
$$\left. + \frac{1}{2}\sqrt{\epsilon_o\left|\frac{\xi}{\Delta}\right|} \sin(z-\pi) \cos\left\{k^*\int \kappa_1\, d\xi - \omega t\right\}\right] \quad . \tag{3.72}$$

## 4. APPROXIMATE SOLUTIONS

We now use the scattering formalism of the preceding section to examine the approximate change in the surface wave as it interacts with the internal current. Using again the notion that if the surface current varies rapidly with position, reflected waves can be generated. If we assume that these reflections are weak, then it is possible to write the reflection matrix in the approximate form given by equation (3.37). These assumptions will be made in the following section, where the reflected wave is calculated in the Born approximation. Section 4B will take into account the variability of the reflected wave amplitude and discuss the eikonal (WKB) solution to the problem. It will be determined that the WKB solutions agree with the solutions obtained for the coupled differential equations [(3.49) and (3.50)] in Section 3C.

### 4A. The Born Approximation

We will now continue the analysis begun in Section 3B, where the scattering of a wave at a boundary is discussed. In this section we assume that the amplitude of the incident wave is constant throughout the interaction. We will further assume that the end points of our propagation interval ($\xi_1$ and $\xi_N$) in Equation (3.30) are very far from the interaction region. Incorporating the single reflection hypothesis in Equation (3.30), taking the continuous limit of the product of the propagation matrices [Equation (3.39)] and using the scattering matrix from Equation (3.36), we may write for the reflected wave,

$$\frac{\phi_{refl}}{\phi_o} \simeq -\sum_j r_j^{(+)}(\xi_j) \exp\left\{i \int^{\xi_j} \left[k^{(+)}(\xi') - k^{(-)}(\xi')\right] d\xi'\right\} . \qquad (4.1)$$

Equation (4.1) is the continuous analogue of Equation (3.38), i.e., because there is only a single scattering from each of the steps ($\xi_j$), the reflected surface wave is a linear superposition of each of these small reflections.

We may write Eq. (4.1) in a more manageable form by taking the limit of the series as an integral in the same spirit as we constructed the propagators [Eq. (3.39)]. To do this, consider the reflection coefficient in Eq. (3.21b), where the wavenumbers $k_A^{(+)}$ and $k_B^{(+)}$ may be more instructively written in terms of the position variable $\xi_j$. We delete the index labeling the region and write the difference in wavenumber at the $j^{th}$ step as

$$k_A^{(+)} - k_B^{(+)} \approx -\left|\xi_{j+1} - \xi_j\right| \left.\frac{dk^{(+)}}{d\xi}\right|_{\xi = \xi_j} \tag{4.2}$$

when the step length $\left|\xi_{j+1} - \xi_j\right|$ is sufficiently small. Using Eq. (4.2) and (3.21b), we may write the reflection coefficient as a function of position

$$r_j^{(+)}(\xi_j) \approx -\frac{\Delta\xi_j}{k^{(+)}(\xi_j) - k^{(-)}(\xi_j)} \left.\frac{dk^{(+)}}{d\xi}\right|_{\xi=\xi_j} . \tag{4.3}$$

Further, since the variation in wavenumber with position is dependent on the variation in the surface current (= βc) with position; it is more natural to write equ. (4.3) as

$$r_j^{(+)}(\xi_j) \approx -\frac{\Delta\xi_j}{k^{(+)}(\xi_j) - k^{(-)}(\xi_j)} \left.\frac{dk^{(+)}}{d\beta}\frac{d\beta}{d\xi}\right|_{\xi=\xi_j} . \tag{4.4}$$

By substituting Equation (4.4) into Equation (4.1) we may express the reflected wave in terms of the integral,

$$\frac{\phi_{refl}}{\phi_o} = \frac{\exp\, ik^* \int^{\xi} \left[\kappa^{(+)}(\xi') - \kappa^{(-)}(\xi')\, d\xi'\right]}{\kappa^{(+)}(\xi) - \kappa^{(-)}(\xi)} \frac{d\kappa^{(+)}}{d\beta} \frac{d\beta}{d\xi}\, d\xi \quad , \qquad (4.5)$$

where the continuous limit of Equation (4.1) has been taken. A further simplification can be made near the resonance condition $\beta \to 0$, $\eta \to 1/4$, i.e., the point where $\kappa_2$ becomes zero in Equation (3.44):

$$\frac{\phi_{refl}}{\phi_o} = \pm \int \frac{\exp\left\{ik^* \int^{\xi} 2\bar{\kappa}\, d\xi'\right\}}{8\bar{\kappa}\, c\, \sqrt{1-4\eta}} \frac{dU}{d\xi}\, d\xi \quad ,$$

where $\bar{\kappa} = [\kappa^{(+)} - \kappa^{(-)}]/2$, and we have used $\eta^2 \sim 1/16$ in an expansion of $\sqrt{1-4\eta}$ .

In the Born approximation the wavenumber $\bar{\kappa}$ is assumed to be a constant throughout the interaction interval and may, therefore, be removed from the integral sign as follows

$$\frac{\phi_{refl}}{\phi_o} = \pm \frac{1}{8\bar{\kappa}\, c\, \sqrt{1-4\eta}} \int_{-\infty}^{\infty} e^{i2k^*\bar{\kappa}\xi} \frac{dU}{d\xi}\, d\xi \quad . \qquad (4.6)$$

We may integrate Equation (4.6) by parts to obtain,

$$\frac{\phi_{refl}}{\phi_o} = \pm \frac{k^*}{4\sqrt{1-4\eta}} \int_{-\infty}^{\infty} \frac{U(\xi)}{c}\, e^{i2k^*\bar{\kappa}\xi}\, d\xi \quad . \qquad (4.7)$$

This is the Bragg condition for scattering, where the reflection from the train of surface currents is proportional to the Fourier component of the surface current distribution at the "mean" wavenumber $2k^*\bar{\kappa}$ . Since at the resonant condition the surface gravity waves are typically of much shorter wavelength than the internal waves, this contribution to the reflection is usually very small.

## 4B. The Eikonal (WKB) Approximation

Of much greater importance than the weak Bragg reflections considered in Section 4A is the possibility of total reflection of the impinging waves, and associated with this, the possibility of trapped waves. To analyze this problem we will use the WKB approximation in the slowly varying regions far from the turning points and match these asymptotic forms to the Airy integral expressions (Section 3D) which are valid in the vicinity of the turning point.

The normal WKB approximation (as used by most workers) permits only one wavenumber to characterize a wave packet and thus must be carefully interpreted when applied to the problem of a wave packet incident on a region having reflecting properties. In the coordinate system moving with the pattern of surface current produced by the internal wave, there are four different propagating waves which may coexist at the same frequency (see Fig. 2 ). Two of these can be strongly coupled if the wave frequency is close to the resonant value (g/4c). Thus, when applying the WKB approximation to this problem it is important to allow for at least two coexistent waves. The effects are most easily deduced from the full wave equation.

We consider first the distortion of the wave as it passes through a region of slowly varying surface currents, described by $U(\xi)$. Thus, at point $\xi$, we have in general for a right traveling wave, using Eqs. (3.1), (3.6) and (3.8),

$$-\omega^2\phi + 2ci\omega\phi_\xi + c^2\phi_{\xi\xi} + 2U(\xi)\left[-i\omega\phi_\xi - c\phi_{\xi\xi}\right] - ig\phi_\xi = 0. \qquad (4.8)$$

We wish to use the WKB approximation to describe the distortion in the interaction region, to this end we introduce the normalized variables from Section 2, and rewrite Equation (4.8) as,

$$\phi_{\xi\xi} + ik^* \frac{2\eta(1-\beta)-1}{1-2\beta}\ \phi_\xi - \frac{\eta^2 k^{*2}}{1-2\beta}\ \phi = 0 \ . \tag{4.9}$$

To gain insight into Equation (4.9) let us put the equation in the following form,

$$\frac{d^2}{d\xi^2}\ (P\phi) + GP\phi = 0 \ . \tag{4.10}$$

Taking the prescribed derivatives and equating terms to those in Equation (4.9) yields for the functions P and G

$$P = \exp\left\{-i\int k^* \kappa_1\ d\xi\right\} \tag{4.11}$$

and

$$G = (k^*\kappa_2)^2 + ik^* \frac{d\kappa_1}{d\xi} \tag{4.12}$$

Therefore, with the substitution $S = P\phi$, we obtain

$$\frac{d^2S}{d\xi^2} + \left[(k^*\kappa_2)^2 + ik^* \frac{d\kappa_1}{d\xi}\right] S = 0 \tag{4.13}$$

for Equation (4.9), which is just that obtained from the coupled differential equations in Section 3C [3.55], when $P\phi$ is the total wave envelope.

In the eikonal or WKB approximation we write S in Equation (4.13) as,

$$S = Ae^{i\Gamma} \tag{4.14}$$

when we require that both the amplitude (A) and phase ($\Gamma$) be real. Substituting Equation (4.14) into (4.13) and equating real and imaginary parts yields the coupled equations,

$$A_{\xi\xi} + \left[(k^*\kappa_2)^2 - \Gamma_\xi^2\right] A = 0 \tag{4.15}$$

and

$$\Gamma_{\xi\xi} + 2\Gamma_\xi\ A_\xi/A + k^* \frac{d\kappa_1}{d\zeta} = 0 \ . \tag{4.16}$$

It is convenient to define $\Gamma_\xi = \kappa$ in the above equations, which may then be written as

$$\kappa^2 = (k^*\kappa_2)^2 + \frac{A_{\xi\xi}}{A} \tag{4.17}$$

and

$$\frac{d}{d\xi}(A^2\kappa) = -k^* \frac{d\kappa_1}{d\xi} A^2 \quad . \tag{4.18}$$

When $\kappa$ is slowly varying over many wavelengths, then we may neglect the second term on the right hand side of Equation (4.17). In this limit (the eikonal approximation)

$$\kappa = \pm k^* \kappa_2(\xi)$$

and

$$\Gamma = \pm \int^{\xi} k^* \kappa_2(\xi')\, d\xi' \quad . \tag{4.19}$$

A second approximation, which is consistent with the analytic treatment in Section 3C is to neglect the contribution of $d\kappa_1/d\xi$ to Equation (4.18). In this case the amplitude varies according to

$$\frac{A(\xi)}{A(\xi_o)} = \sqrt{\frac{\kappa_2(\xi_o)}{\kappa_2(\xi)}} \tag{4.20}$$

which results from the approximation

$$\frac{d}{d\xi}(A^2\kappa) \approx 0 \quad .$$

Using these results in conjunction with Equations (4.14) and (4.11) we may write the envelope of the wave potential in the form,

$$\frac{\phi}{\phi_o} = \sqrt{\frac{\kappa_2(\xi_o)}{\kappa_2(\xi)}} \exp\left\{ i \int^{\xi} k^* \left[ \kappa_1(\xi') \pm \kappa_2(\xi') \right] d\xi' - i\omega t \right\} \tag{4.21}$$

where $\phi_o$ is the initial amplitude. The wave height at a point $\xi$ with reference

to the height at the point $\xi_o$ where the current $[U(\xi)]$ vanishes, is given by

$$\frac{y}{y_o} = \left(\frac{U_o}{U_o - U(\xi)}\right)^{1/4} \exp\left\{i\int_{\xi_o}^{\xi} k^*\left[\kappa_1(\xi') \pm \kappa_2(\xi')\right]d\xi' - i\omega t\right\} \qquad (4.22)$$

where $\kappa_1$ and $\kappa_2$ may be obtained from Equation (3.45). Equation (4.21) is in essential agreement with the asymptotic expression in Equation (3.69) when a linear current profile is assumed and when we identify the + sign with $\phi^{(+)}$ and the minus sign with $\phi^{(-)}$. Thus we may take the general solution to be given by

$$\phi = \phi^{(+)} + \phi^{(-)}$$

where $\phi^{(+)}$ and $\phi^{(-)}$ are given by Equation (4.21), except in the vicinity of the turning point. In this latter region, we must use the full wave expression (Eqs. 3.63 and 3.65).

## 5. DISCUSSION AND CONCLUSIONS

This section is divided into three parts. The first part summarizes the mathematical structure of the paper stressing the various assumptions employed. A descriptive summary of the physical mechanisms involved in the scattering process based on analogy with balls rolling on slowly-varying potential surfaces is provided in the second subsection. The third subsection discusses the phenomenon of surface modifications produced by weak currents and presents exemplary calculations of the modifications expected for a 'linear' sea.

### 5A. Summary of the Formal Structure

In Figure 9 we indicate diagramatically the major content and structure of the mathematical analysis developed in Sections 3 and 4. The general hydrodynamic equation for the ocean surface

$$\left[\Phi_{tt} + (\nabla\Phi\cdot\nabla\Phi)_t + \frac{1}{2}\nabla\Phi\cdot\nabla(\nabla\Phi\cdot\nabla\Phi) + g\Phi_y\right]_{surface} = 0 \qquad (5.1a)$$

is used to model the interaction between surface gravity waves and low speed, low amplitude surface currents. This is done by assuming the velocity potential to be of the form $\Phi = \phi + \Phi^{(o)}$, where $U(\vec{x},t) = \nabla\Phi^{(o)}$ is the weak surface current and $\phi$ is the velocity potential for the surface gravity waves. Equation (5.1) is linearized by taking the ratio of the gravity wavelength to the current wavelength $(\lambda_{wave}/\lambda_{current}) << 1$, so that in one horizontal dimension we obtain

$$\phi_{tt} + g\phi_y + 2U(x,t)\phi_{xt} \approx 0 \quad . \qquad (5.1b)$$

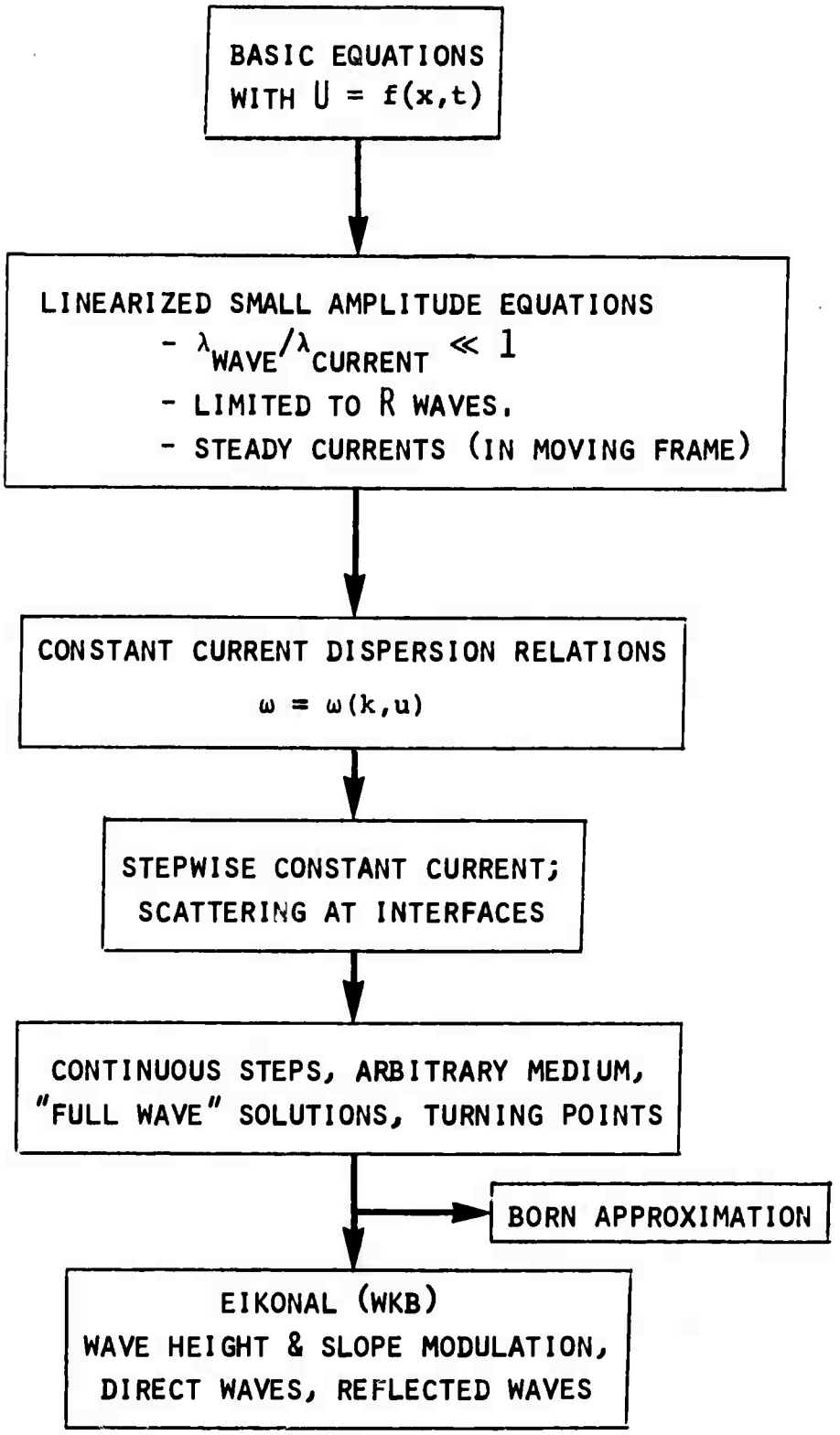


FIGURE 9. STRUCTURE OF THE MATHEMATICAL DEVELOPMENT

Equation (5.1b) has a first order interaction term involving a prespecified, non-uniform surface current.

There are a number of possible causes of the surface current, e.g., general ocean circulation, swells, river inlets, internal waves, etc. If we assume that the current is the result of an internal wave propagating along a thermocline, the situation is unique in that, in the coordinate system travelling with the internal wave, the surface current pattern is stationary (so long as the internal wave is non-dispersive). In this coordinate sytem ($\xi = x - ct$) there exist four possible co-existing waves, two of which have a positive and two of which have a negative phase velocity [see Figure (4)]. The two waves with positive phase velocities (right moving or R-waves), have a dispersion relation (for constant current $U_o$)

$$-\eta^2 - 2\eta\kappa - \kappa^2 + 2\beta_o\left[\eta + \kappa\right]\kappa + \kappa = 0 \qquad (5.2)$$

in terms of the normalized frequency ($\eta = c\omega/g$), wavenumber ($\kappa = kc^2/g$) and current ($\beta_o = U_o/c$). These two waves have opposing group velocities ($d\omega/d\kappa = d\eta/d\kappa = c_g$), however, and our discussion centers on the interdependence of these two waves ($\phi^{(+)}$ and $\phi^{(-)}$ waves). In the case of a steady current [$U(\xi)$], this description leads in a natural way to the notion of incident and reflected waves from the weak current region.

From the above dispersion relation [Equation (5.2)] it is possible to determine the wave frequency in terms of the wavenumber and current amplitude. At the point where the group velocity of the R-wave vanishes ($c_g = d\eta/d\kappa = 0$) the surface wave travels in synchronism with the internal wave and the $\phi^{(+)}$ and $\phi^{(-)}$ waves are strongly coupled. This condition for strong coupling can be expressed in terms of

critical values for the current, via the dispersion relation. These concepts are formulated mathematically in Section 3B by considering a stepwise constant current. Each step is treated as a boundary and the incident wave is partially reflected and partially transmitted at each boundary. By requiring continuity of amplitude and slope of the transmitted and reflected waves at each of these steps, a scattering matrix for the current region may be developed. The continuous limit of these equations using the assumption of a weakly reflecting current is taken in Section 3C. This leads to a set of coupled partial differential equations for $\phi^{(+)}$ and $\phi^{(-)}$. The coupling is dependent on both the current and the spatial gradient of the current.

The above set of coupled differential equations [Equations (3.49) and (3.50)] may be reduced to a single equation for the wave envelope, i.e., $S \sim \phi^{(+)} + \phi^{(-)}$, [Equation (3.55)]. This equation becomes an Airy integral for a linear current profile when the distance from the reflection point is much greater than the characteristic wavelength of the gravity waves.

In Section 4 the connection between the scattering approach to the interaction problem is compared with a straightforward treatment of the linearized dynamic equations [Equation (5.1b)]. A little algebra establishes that in the moving coordinate system

$$\frac{d^2S}{d\xi^2} + (\alpha_1 + i\alpha_2)S = 0 \qquad (5.3)$$

where S is the wave envelope as defined in Section 3. The scattering theory, therefore, yields the same dynamic equation for the interaction problem as linearizing Equation (5.1).

Equation (5.3) is solved in the WKB solution under the condition that $\alpha_1 >> \alpha_2$, which is the same condition used in Section 3. The WKB solutions are identical to the asymptotic forms obtained in Section 3 when a linear profile for the current is assumed. The turning points in the WKB solutions, i.e., the points where the wave amplitude becomes infinite, are the spectral or total reflection points for the incident wave. This is discussed more fully in Section 5C.

5B. Interpretation in terms of the scattering of wave packets.

The above summary of the formalism has shown that the two models - (i) the linearized hydrodynamic equation for the ocean surface, and (ii) the notion of weak reflections of the surface gravity waves by the surface current - imply the same dynamic description of the interactive process. The importance of the present description of the process lies in the physical insight that it provides. We see that, just as in the scattering of electromagnetic waves from a region of varying refractive index or scattering of a quantum mechanical wave (i.e., a particle) from a potential well, it is possible to interpret this linearized ocean wave-current interaction model in terms of scattering theory.

Under certain circumstances the scattering can be very strong (resonant). The interaction has a close formal analogy with scattering of particles by a shallow potential well. In order to give a physical description of the type of resonance involved, we describe the analogous resonance which occurs in scattering of particles by a shallow potential well and make reference to the text where appropriate.

Think of a tightly stretched rubber sheet, and of a very slight hill travelling at constant speed ($v_{hill}$) across this sheet (as would be created by a moving finger pushing the sheet up just slightly from below). The hill is the surface current distribution ($v_{hill} = c_{phase}$) created by the internal wave. We now shoot marbles at the moving hill. The marbles are the short wavelength surface gravity waves ($v_{marble} = c_g$). A marble moving very fast will not be much affected by the hill except for feeling it as a brief faint bump. A marble moving very slowly will also not be affected very much since the hill will overtake it and pass it too quickly to cause much motion. However, a marble that moves almost at the same velocity as the hill feels its presence for a long time and can interact strongly. This is the resonance. For low hills a perturbation theory could be used to describe the interaction, but the results would blow up when $v_{hill} = v_{marble}$ [Equation (2.26)], giving a perturbation growing linearly in time [Equation (2.28)] (this is essentially the Hartle-Zachariason calculation for the wave-wave interaction). In this model (at least in a <u>one</u>-dimensional model), it can be shown that there is a specific, sharply bounded range of marble velocities centered around $v_{hill}$ for which the interaction is strong and that outside this range the interaction is weak. In this velocity range the marbles lose or gain energy as they hit or are hit by

the hill. The effect is most easily understood by viewing it in a coordinate system moving with the hill (remember this is one dimension so that the hill is more like a long ridge). In this coordinate system the hill (internal wave current) does not move. Marbles (short gravities) overtaking the hill appear now to come from the left whereas marbles being overtaken by the moving hill appear to impinge from the right. The impact velocity is $\pm (v_{marble} - v_{hill}) = \pm|\Delta v|$ (see Section 1). For large $|\Delta v|$ the marble slows down slightly as it climbs the hill, but regains its original velocity as it rolls down the other side. However, there is a critical value of $\Delta v (= \Delta v^*)$, dependent on the hill height $(A_o)$, below which marbles cannot get over the hill - they are reflected. In the ocean-fixed coordinate frame, these marbles gain or lose a velocity $\pm 2\Delta v$. The interaction is very strong for marbles having velocities in this range $(v_{hill} \pm \Delta v^*(A_o))$, i.e., <u>every</u> such collision results in a (group) velocity change of $\pm 2\Delta v$.

In particular, it is to be noted that <u>no</u> marbles which have a velocity in the range $v_{hill} \pm \Delta v^*(A_o)$ are ever found on or near the top of the hill - they are always reflected away.

For a given internal wave having speed c and amplitude $A_o$, there is a specific range ($\lambda_1$ to $\lambda_2$) of wavelengths of surface gravity waves which are strongly reflected by the current pattern of the internal wave. That is, for $\lambda_1 < \lambda < \lambda_2$, waves obeying

$$\left| c - \frac{1}{2}\sqrt{g\lambda/2\pi} \right| < \Delta v^*(A_o)$$

cannot exist at the top of the internal wave. Such wavelengths should be absent or at least strongly altered in the wave amplitude power spectrum and therefore also in the radar return in certain regions over the internal wave.

## 5C. Application to the Mechanical Generation of 'Slicks'

In this section we provide estimates of the range of frequencies and wavenumbers which are predicted to be strongly altered by a given internal wave. Also, examples of the spatial modulation of a wave spectrum are evaluated for a 'linear' sea.

For a finite packet of roughly sinusoidal currents having a peak amplitude $A_o$, the frequencies which can be reflected, i.e., for which there are turning points, should be in a range

$$\eta = \frac{1}{4} \pm \frac{A_o}{c} \tag{5.5a}$$

that is,

$$\omega = \frac{g}{4c} \pm \frac{1}{4} \frac{gA_o}{c^2} \quad . \tag{5.5b}$$

These are wave frequencies as seen in the moving coordinate system. The corresponding wavenumber range (outside the current region) can be obtained from the dispersion relation for the unperturbed ocean:

$$\frac{kc^2}{g} = \kappa = \frac{1-2\eta}{2} \pm \frac{1}{2}\sqrt{1-4\eta} \simeq \frac{1}{4} \pm \frac{1}{2}\sqrt{1-4\eta} \quad . \tag{5.6}$$

Thus, waves in the free ocean that have wavenumbers in the range

$$|k - k_R| \leq 2k_R\sqrt{A_o/c} \tag{5.7}$$

(where $k_R$ is the wavenumber of the resonance [$c_g(k_R) = c$])will be reflected (i.e., reverse their group velocity as seen in the moving coordinate system) by the surface currents. In the ocean-fixed coordinate system waves having these wavenumbers do not in general reverse direction but appear to interact strongly with the current region.

The variation of the wavenumber with position in the current pattern can be followed with the aid of Figure 10. Here we have plotted the value of the reduced wavenumber $\kappa$ as a function of the local value of the reduced current ($\beta$) for various fixed frequencies ($\eta$ = constant). In this plot the unperturbed ocean is the vertical axis $\beta = 0$ and the point representing a given wave packet moves along one of the curves $\eta$ = constant as the wave packet traverses the current region. Reflected waves are those which return to the $\beta = 0$ axis at a value of $\kappa$ different from the initial value. For example, according to Figure 10, waves having an unperturbed (reduced) frequency $\eta = 0.24$ can be reflected if $\beta$ dips below - 0.04. Viewed from the ocean-fixed coordinate system, these waves change their wavenumbers as a result of a "collision" with a turning point:

$$\left| \frac{\Delta k}{k} \right| \leq 2\sqrt{A_o/c}$$

and lose or gain velocity

$$\left| \frac{\Delta c_g}{c_g} \right| \leq \sqrt{A_o/c} \quad .$$

The mean square amplitude is unchanged (in this one-dimensional problem), but the mean square slope can change within the limits:

$$\left| \frac{\Delta(ka)^2}{(ka)^2} \right| \leq 4\sqrt{A_o/c} \quad .$$

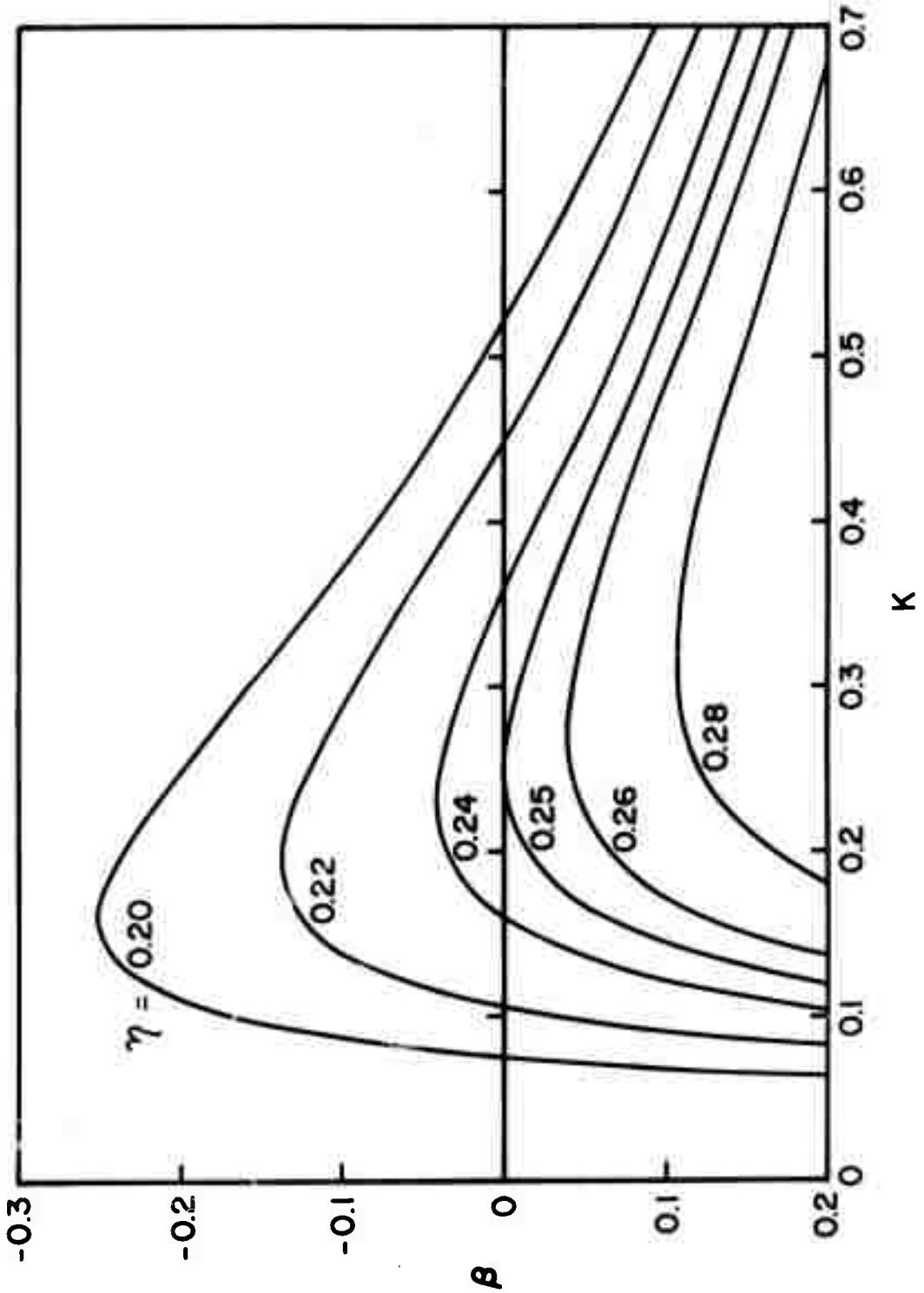


FIGURE 10. REDUCED WAVENUMBER $\kappa(=c^2k/G)$ AS A FUNCTION OF THE CURRENT PARAMETER $\beta$ $(=\Delta U/c)$ FOR FIXED VALUES OF THE FREQUENCY $\eta(=c\omega/G)$

These changes are the "residual" changes that remain after the wave has ceased interacting with the current pattern. The changes that take place during the course of the interaction can differ considerably from these values. However, even these residual values can be significant. Consider a long wavelength internal wave propagagating at 0.5 meters/second along a thermocline at 50 meters depth. An amplitude of the internal wave of one meter would create a surface current that oscillates between $\pm$ 1.0 centimeters/second. This current would (in the absence of non-linear effects) be capable of strongly interacting with surface waves having wavelengths between 50 and 75 cm. The most strongly-altered waves would have their wavelengths changed by up to 40%, their group velocity by up to 20%, and their mean square slopes by up to 80%.

As indicated above, the moving current pattern associated with a travelling internal wave modifies the spectral distribution of surface waves in two ways. Within the region of finite current gradient, the wave amplitudes and slopes are altered according to Equations (3.49) and (3.50). In addition to this local effect, some of the waves intercepted by the current pattern are modified by the scattering process described in Section 3 and leave the region of interaction with altered wave speeds. As these reflected waves propagate away from the current pattern, they alter the spectral distributions at distances remote from the scattering region. To demonstrate these effects, we consider the effect of the passage of a simple gaussian-shaped internal wave packet of peak amplitude $\underline{a}$ travelling along

a sharply-defined thermocline at depth D (Figure 11). The surface current has the form

$$\frac{\Delta U}{C_o} = \beta = -\frac{a}{D} \exp\left(-(x - C_o t)^2/\Delta^2\right) \quad . \tag{5.8}$$

and we evaluate the steady state spectral distribution at differing spatial locations relative to the current packet.

In the frame of the internal wave, R-waves impinge from both directions: "(+)" waves, corresponding to wave packets moving in the positive direction and having group velocities greater than that of the internal wave, and "(-)" waves, corresponding to those moving slower than the internal wave. In Figure 12 we show x - t plots of wave packet trajectories. The waves that are reflected by the current regions appear as discrete bundles in these plots.

To demonstrate the modification of a spectrum of linear waves by a travelling current pattern, we assume that the incident waves have a $k^{-3}$ spectrum. This spectral form is chosen to simulate that of a saturated sea, although it is recognized that this linear wave model is not consistent with the concept of a sea limited by non-linear effects. In Figure 13 we show the calculated power spectrum (multiplied by $k^3$) at three different points: one ahead of, one behind, and one directly over the internal wave. These results were obtained using the WKB approximation formulas (Equations 4.21 and 4.22) with the standing wave pattern created by the reflected wave smeared out. The data are presented in terms of dimensionless variables and can be scaled to various conditions. For example, for an internal wave velocity of 50 cm/sec, the resonant wavenumber, frequency, and wavelength are: $k = 0.097\ cm^{-1}$, $\omega = 9.8\ sec^{-1}$,

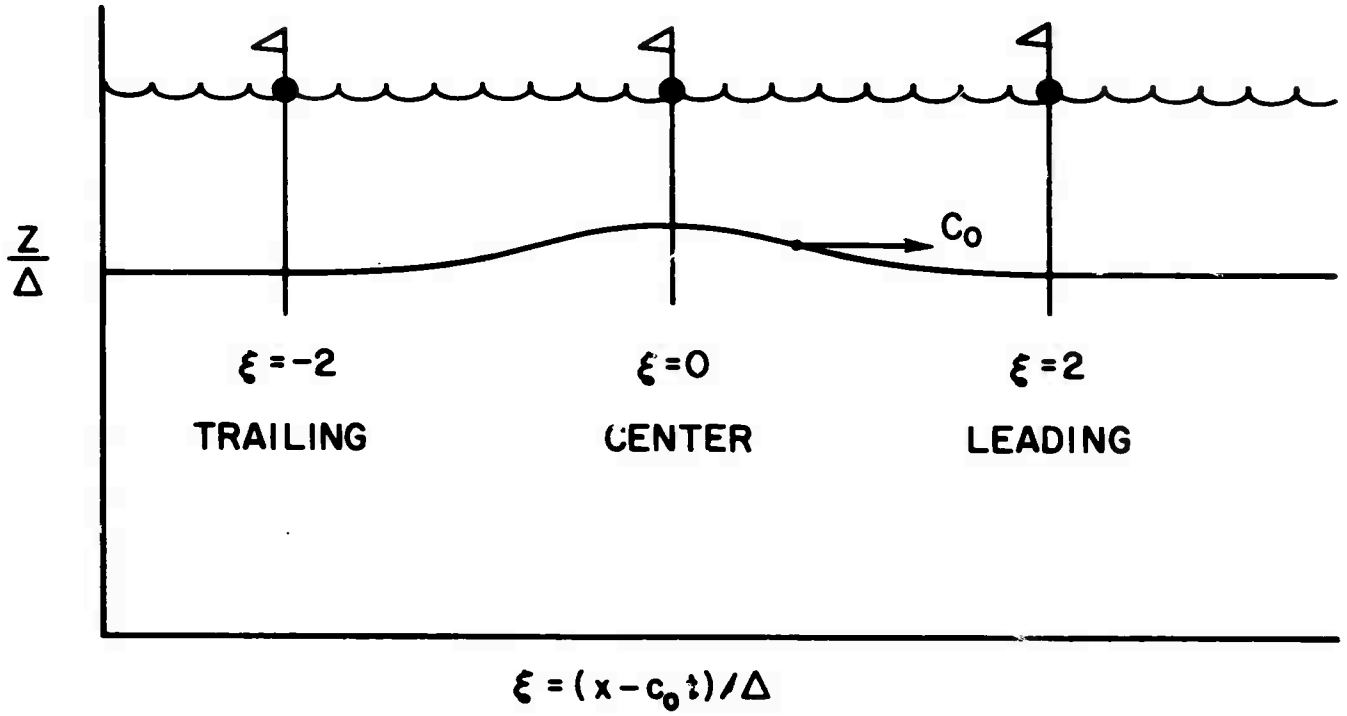


FIGURE 11. GEOMETRY FOR WAVE SPECTRA CALCULATIONS

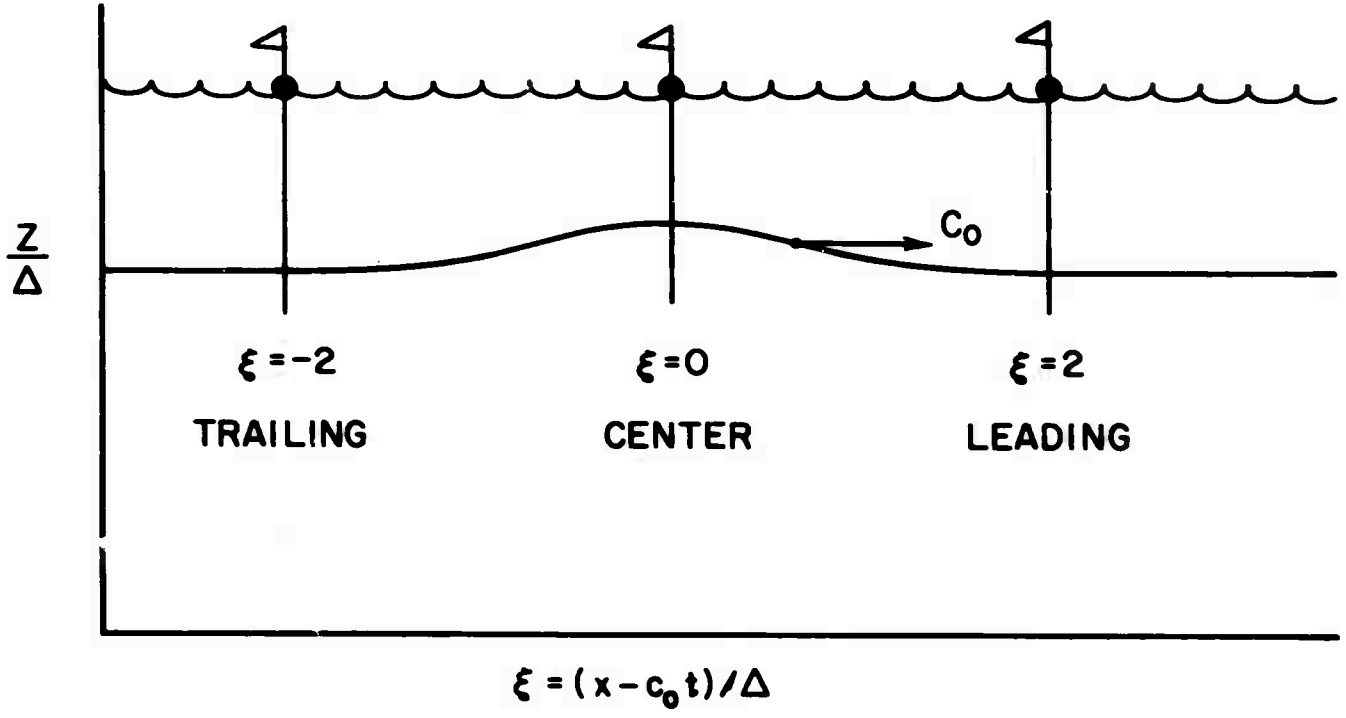


FIGURE 11. GEOMETRY FOR WAVE SPECTRA CALCULATIONS

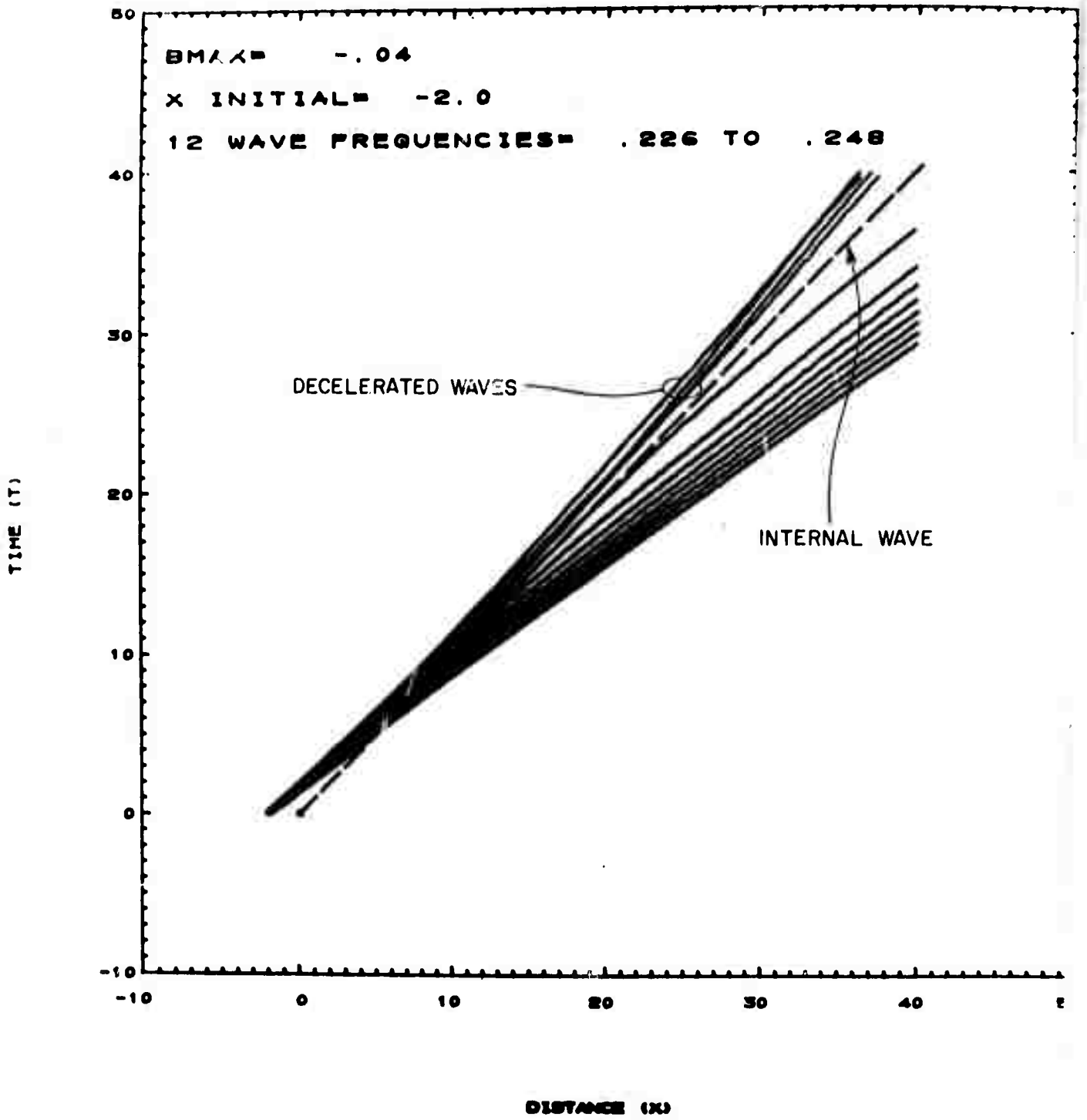


FIGURE 12A. SPACE-TIME TRAJECTORIES FOR THE STRONGLY INTERACTING GRAVITY WAVES ($\phi$ (+) WAVES)

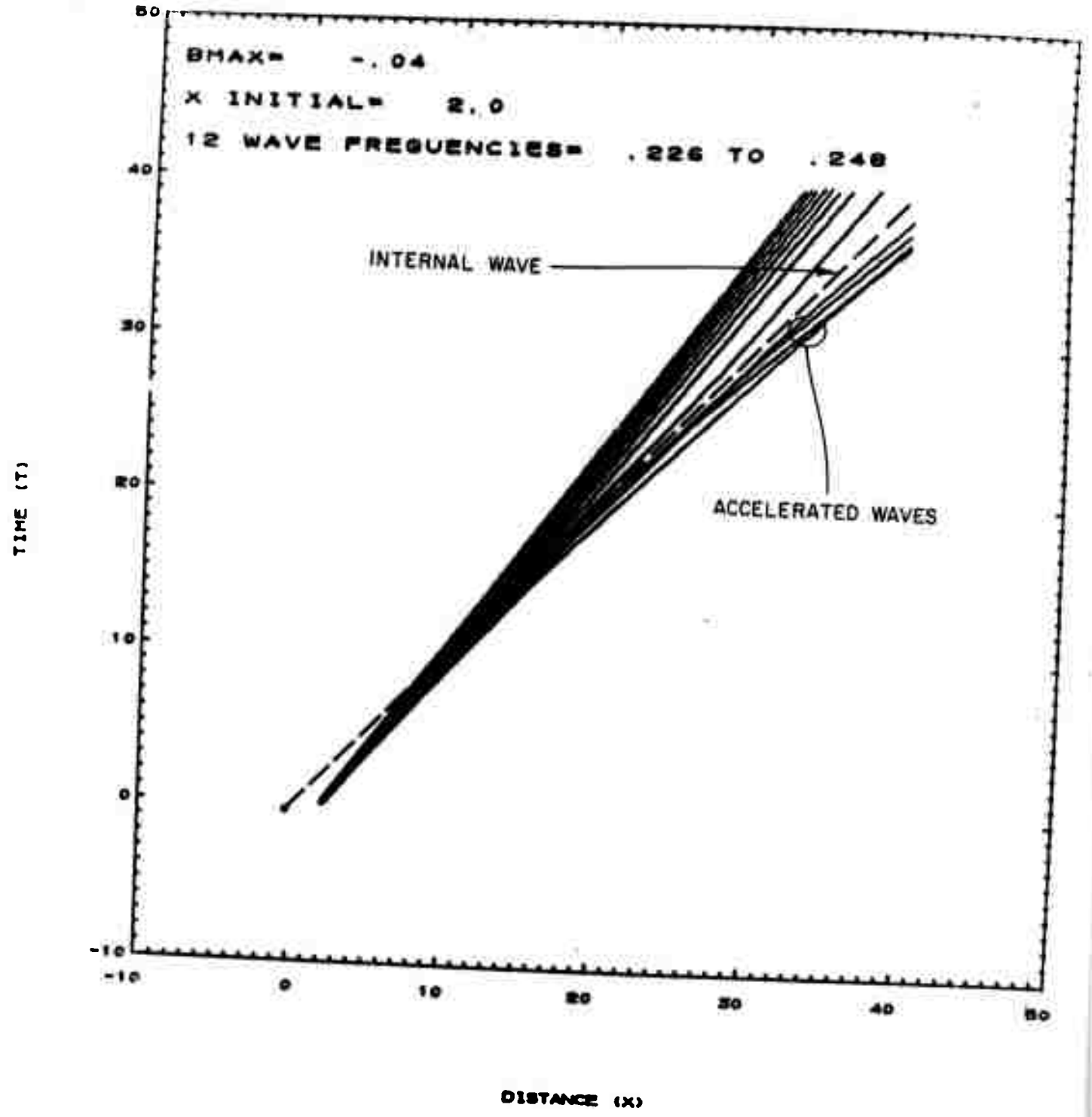


FIGURE 12B. SPACE-TIME TRAJECTORIES FOR THE STRONGLY INTERACTING GRAVITY WAVES ($\phi^{(-)}$ WAVES)

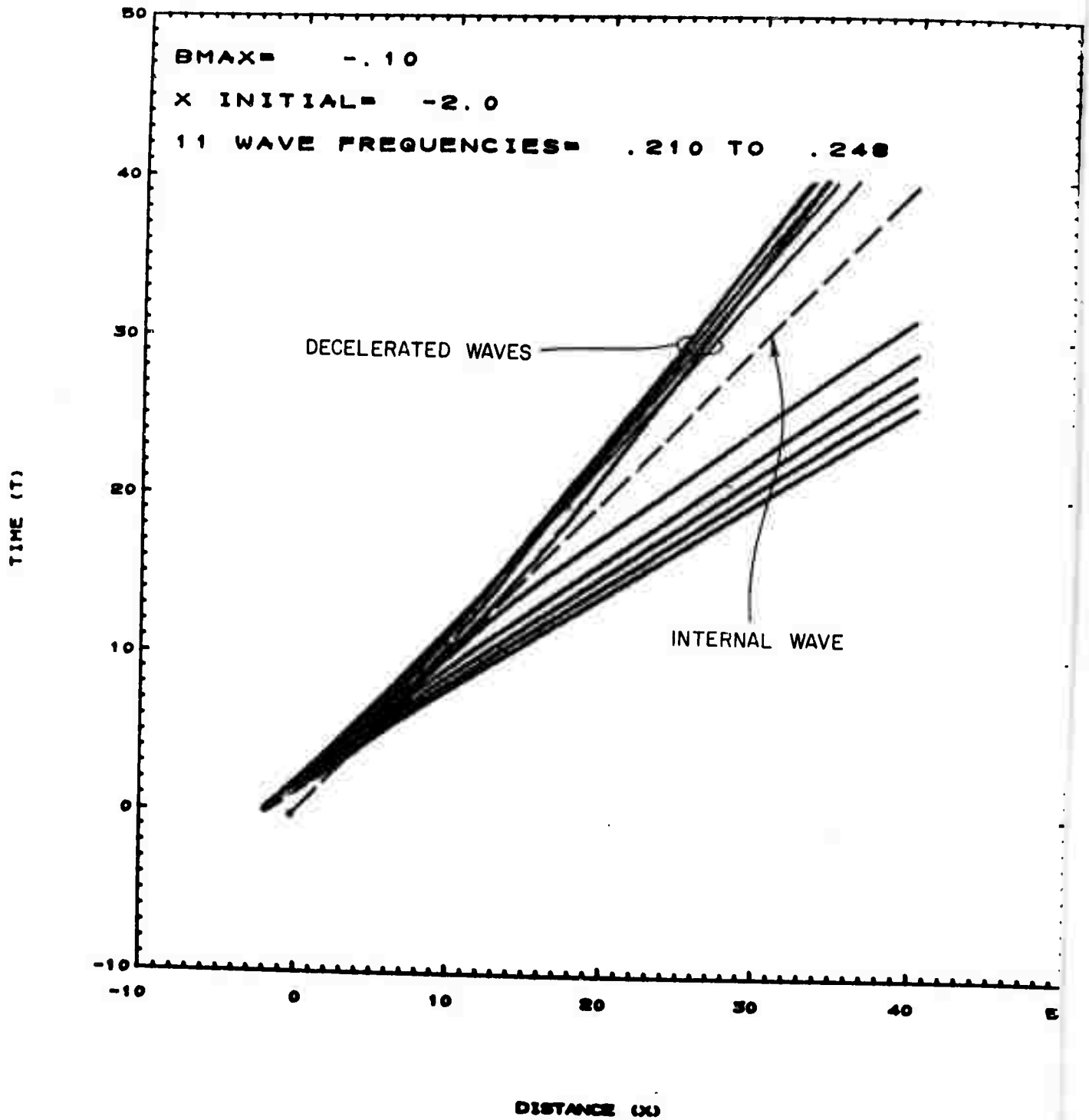


FIGURE 12c. SPACE-TIME TRAJECTORIES FOR THE STRONGLY INTERACTING GRAVITY WAVES ($\phi^{(+)}$ WAVES)

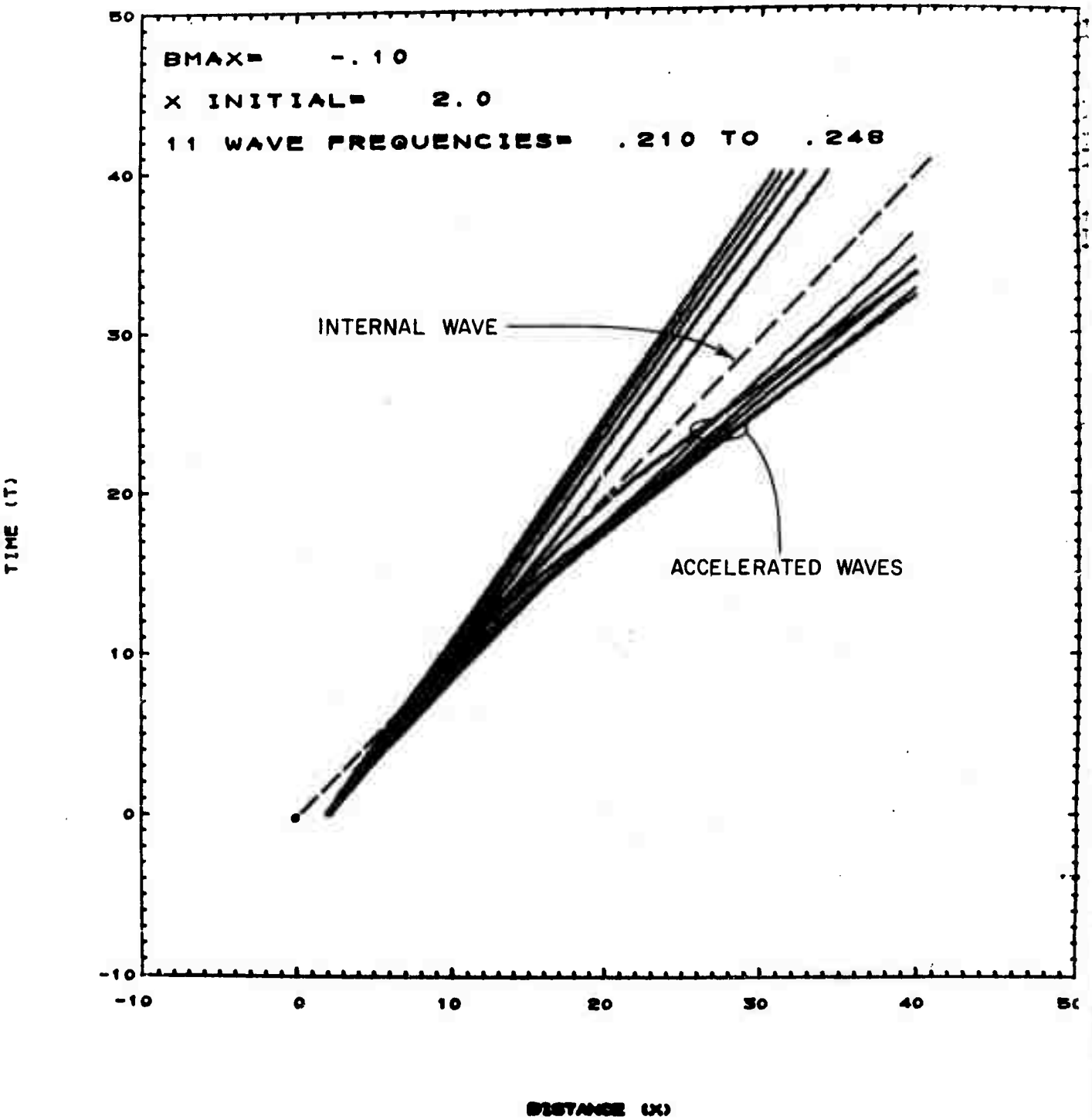


FIGURE 12D. SPACE-TIME TRAJECTORIES FOR THE STRONGLY INTERACTING GRAVITY WAVES ($\phi^{(-)}$ WAVES)

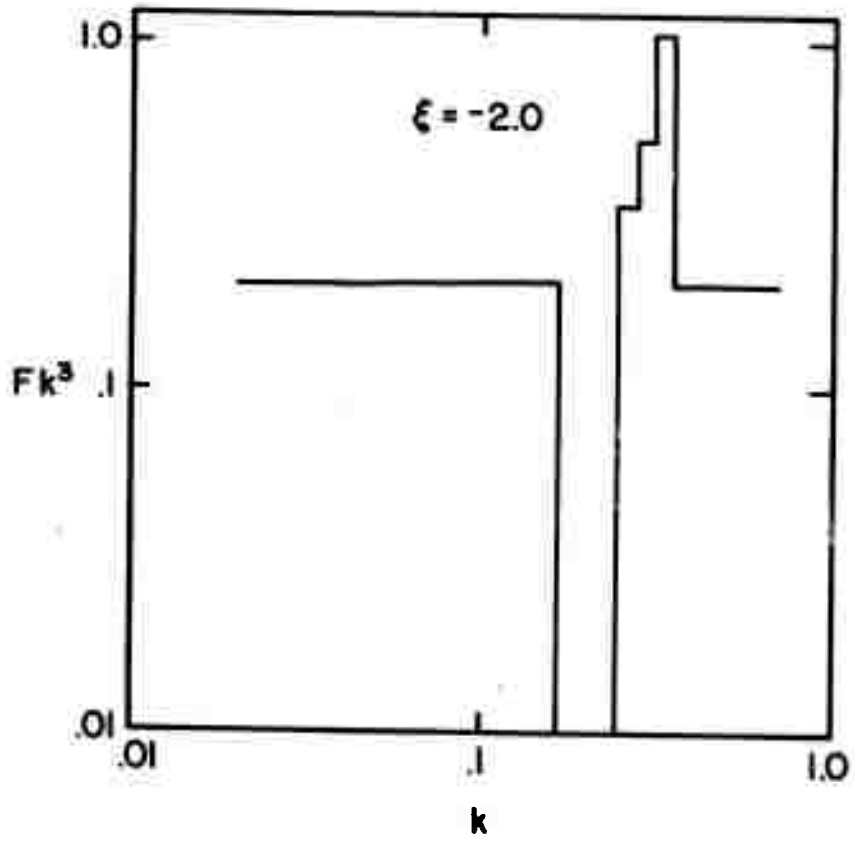


FIGURE 13A. SURFACE WAVE HEIGHT SPECTRUM (TIMES $K^3$) AT A POINT BEHIND THE INTERNAL WAVE FOR $\beta_{MAX} = -0.04$ ($Fk^3$ IS NORMALIZED TO THE VALUE 0.20 IN THE UNPERTURBED OCEAN)

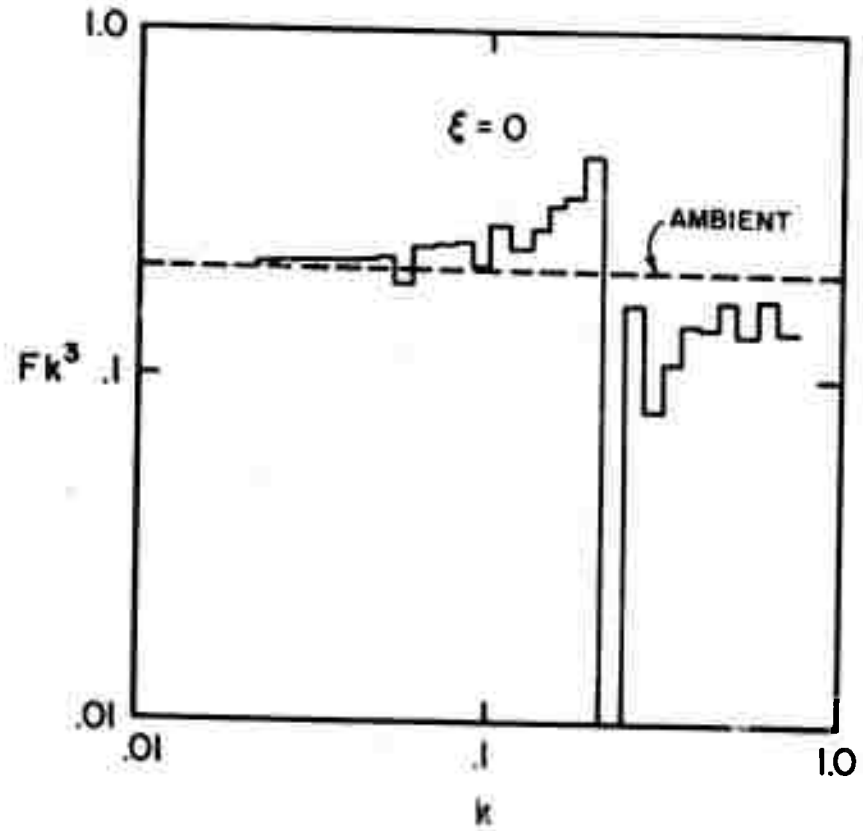


FIGURE 13B. SURFACE WAVE HEIGHT SPECTRUM (TIMES $K^3$) DIRECTLY OVER THE CREST OF THE INTERNAL WAVE ($\beta_{MAX} = -0.04$)

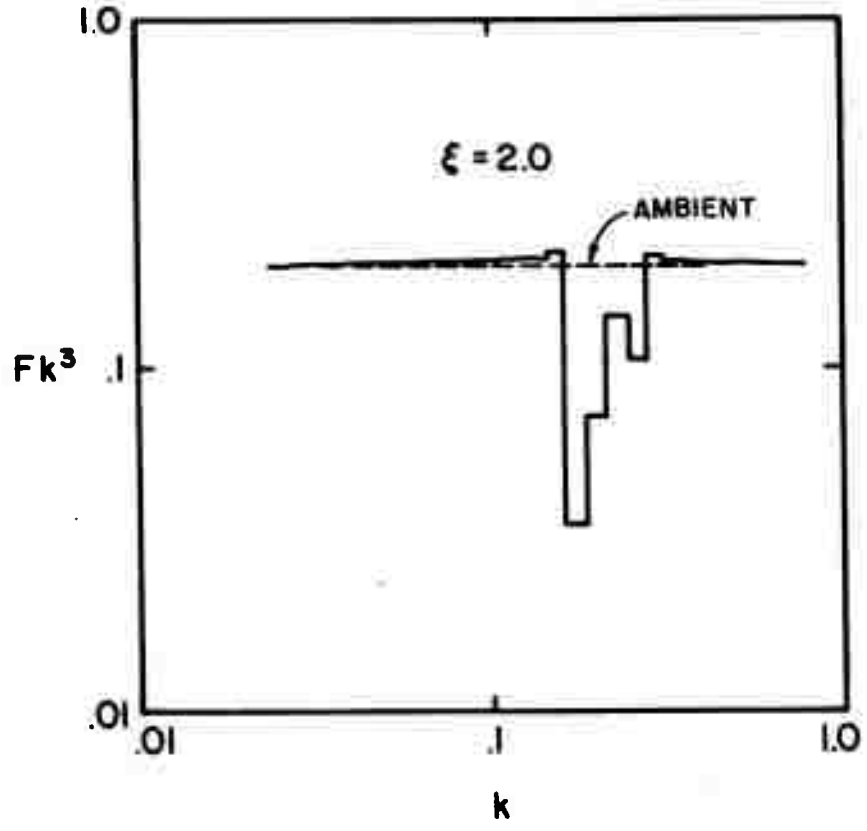


FIGURE 13c. SURFACE WAVE HEIGHT SPECTRUM (TIMES $k^3$) AHEAD OF THE INTERNAL WAVE ($\beta_{MAX} = -0.04$)

$\lambda$ = 64 cm (corresponding to the dimensionless values $\kappa$ = 0.25 and $\eta$ = 0.25.). For the example chosen ($\beta$ = - 0.04), the surface current varies from zero to - 2.0 cm/sec over the crest of the wave.

The calculation shows a number of interesting effects. First, over the internal wave crest (Figure 13b), the spectrum is distorted over a rather broad range of wavenumbers. The broadening is less ahead or behind the internal wave (where it is consistent with approximate estimates given earlier).

Another effect noticeable is the lack of intense caustic formation. Although a single wave incident on the pattern would show a large amplitude enhancement (infinite in this approximation) in the neighborhood of its turning point, this is not true when the incident waves are spectrally distributed. Here, because different wave packets have turning points at different locations, the net effect on the spectrum is a finite distortion (see Figure 13b).

Outside the current region we see the effect of reflected waves. In front of the internal wave the net effect is an apparent depletion of the high wavenumbers (a "smoothing"). This results from the fact that, as the surface waves are overtaken by the internal wave, those that are "blocked" by the current are accelerated and move ahead of the current pattern with decreased wavenumber (increased wavelength). Because the spectrum falls off rapidly with increasing wavenumber, the resulting depletion at high wavenumbers is much more noticeable than the corresponding increase at low wavenumbers.

The opposite effect occurs astern of the internal wave. Here the reflection process increases the wavenumber resulting in a strong increase in the high wavenumber part of the spectrum as compared to a fractionally-

weaker decrease in the low wavenumber part. Thus this linear model would predict an apparent high wavenumber smoothing ahead of the internal wave crest and a roughening astern. Directly over the crest both effects occur: low wavenumbers are enhanced, high wavenumbers are suppressed.

The morphology discussed above applies to a linear sea. Non-linear effects in the real ocean can be expected to severely limit the magnitude of the effects induced; however, the morphology should be similar. That is, a region of advancing positive current gradient (such as that over the bow of an internal wave crest) tends to accelerate the near resonant waves and results in a depletion of the high wavenumber portion of the spectrum (a "smoothing"). An advancing region of negative current gradient (such as in the convergence zone trailing an internal wave crest) leads to enhancement of high wavenumbers (a "roughening").

One can infer some of the real ocean effects by following the motion of an individual wave packet as it traverses the variable current region. In Figure 14 we show histories of a wave packet as it enters the current pattern and is reflected. The mean square amplitude enhancement and mean square slope enhancement are plotted as a function of time. In a truly linear sea, the amplitude and slope enhancement depend solely on the local value of the current and is maximum when the group velocity relative to the internal wave vanishes.

The enhancements shown in Figure 14 are much larger than can be expected to occur in a fully-developed sea, however. A rough estimate of

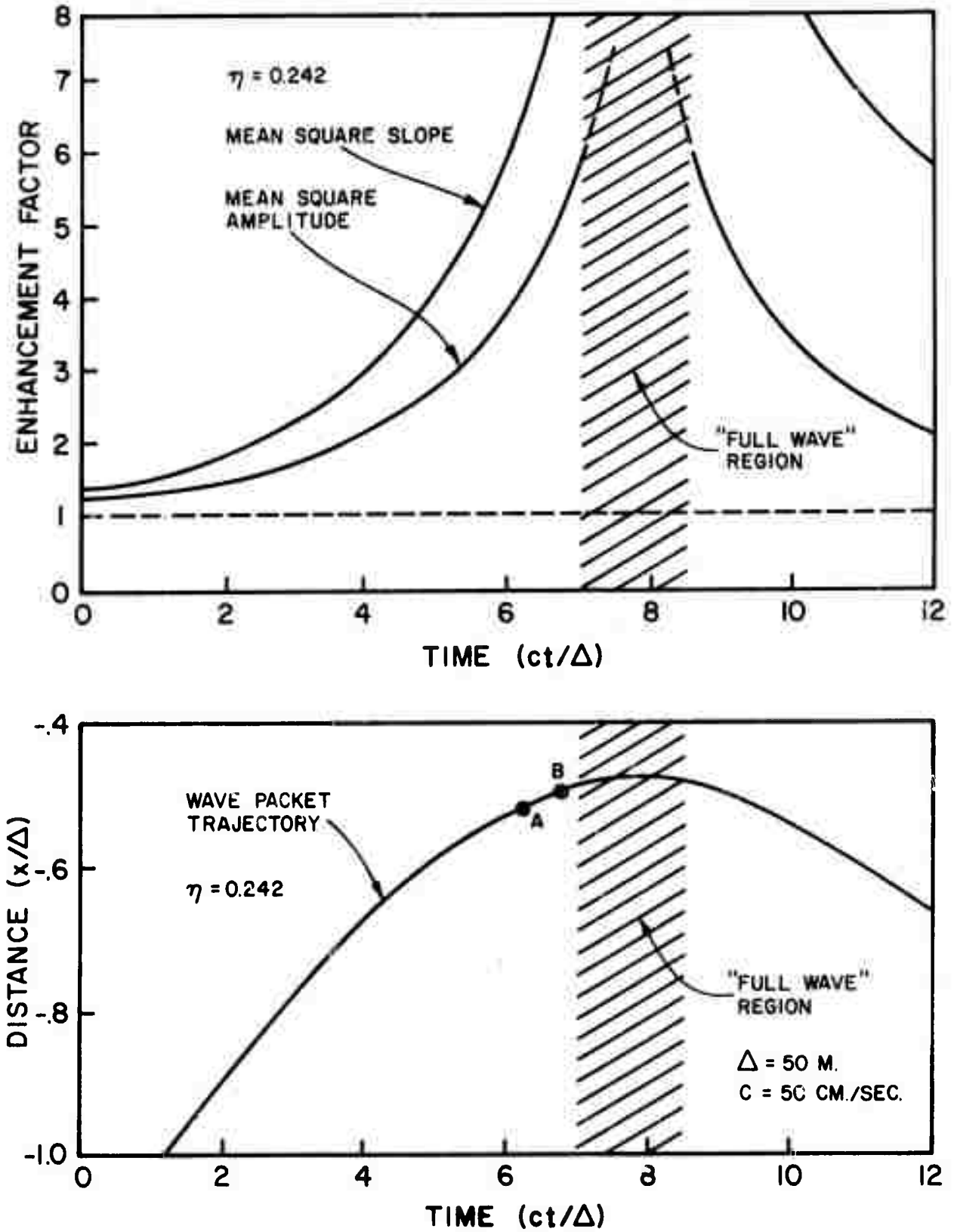


FIGURE 14. ENHANCEMENT FACTORS AND TRAJECTORY FOR A WAVE PACKET HAVING AN UNPERTURBED WAVELENGTH OF 95 CM (THE RESONANT WAVELENGTH IS 64 CM). DISTANCE IS MEASURED FROM THE INTERNAL WAVE CREST.

the real ocean effects to be expected can be obtained by introducing the concept of a coherence time. This is the time required for wind, wave-wave, or dissipative interactions to alter the wave under consideration. Rough estimates of this time (measured in wave periods) are shown in Figure 15 and indicate that coherence times in the range of 10 to 100 wave periods are typical for a saturated sea. The wind interaction time was estimated from Phillips (1966). Two estimates are given for the non-linear wave interaction time; the upper one according to Benjamin (1967) [$\tau/T = k^2a^2/\pi$ and $k^2a^2 \sim 0.006$ for a saturated sea] and the lower one according to Hasselman (1967) [$\tau/T \sim \overline{\nabla\zeta^2}$ with the mean square slope $\overline{\nabla\zeta^2}$ fitted to the data of Cox and Munk].

For example, consider the gaussian-shaped internal wave discussed previously. This wave had a half width $\Delta$ = 50 meters, a peak amplitude a = 2 meters, and was assumed to be travelling at 50 cm/sec along a sharp thermocline at 50 meters depth. We follow a surface wave which, in the unperturbed ocean, has a wave length equal to 95 centimeters (wave period of 0.78 sec.) and which travels at a group velocity equal to 60.8 cm/sec (i.e., it is overtaking the internal wave at an initial relative velocity of 10.8 cm/sec).

According to Figure 14 this wave will be decelerated to the internal wave speed by the time it has penetrated to a point 24 meters behind the internal wave crest. For such a wave the width of the "full wave" region (as defined by the point where the Airy integral argument $\zeta$ is equal to unity - see Eq. 3.59) is given by the expression

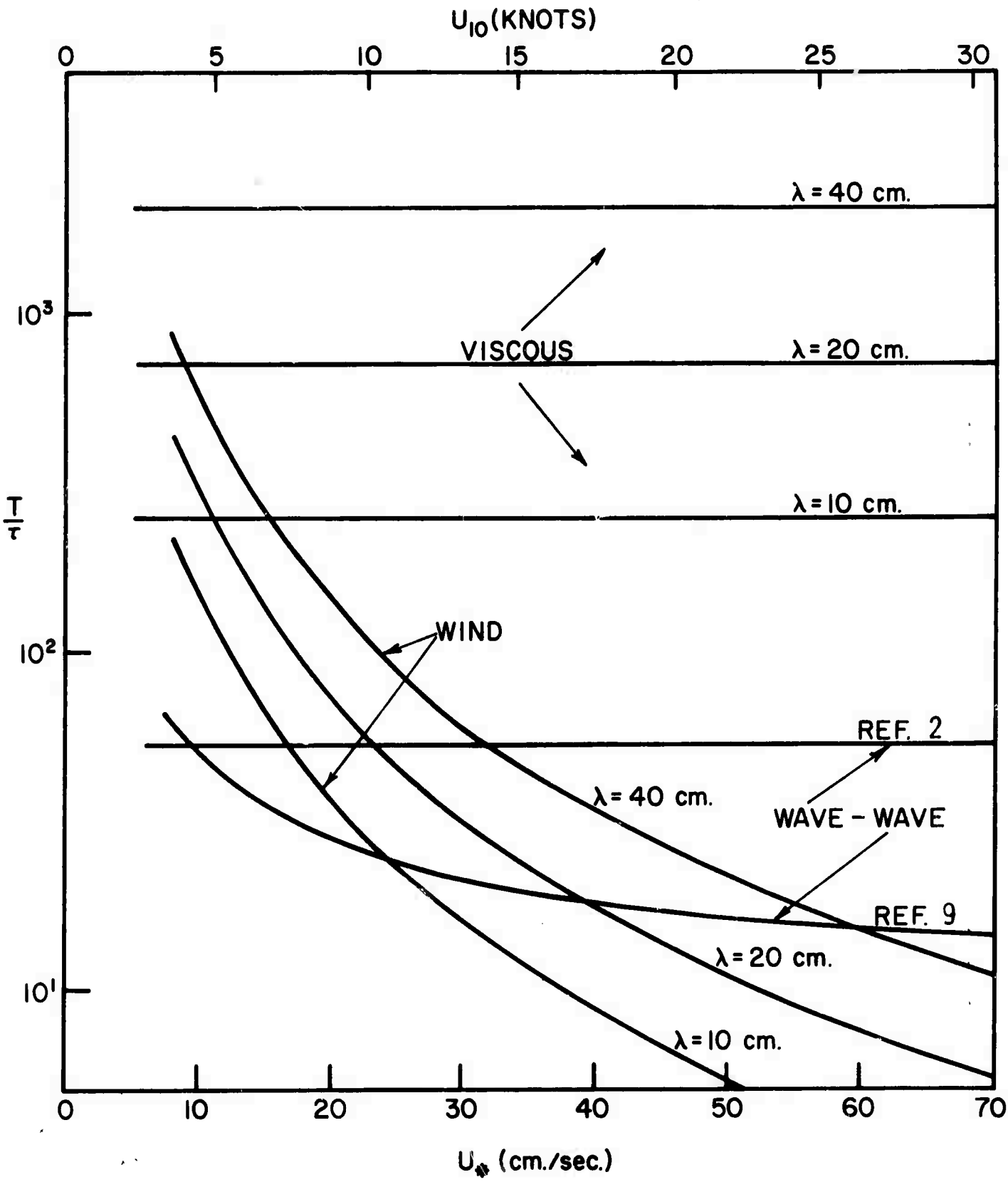


FIGURE 15. ESTIMATED INTERACTION TIMES FOR VARIOUS EFFECTS. HERE U* IS THE TURBULENT FRICTION VELOCITY AND $\tau$ THE WAVE PERIOD.

$$\Delta x \doteq \left[4c/(k^2 du/dx)\right]^{1/3}$$

where du/dx is the local current gradient. At the reflection point in our example, the current gradient is about $-4 \times 10^{-4}$ $sec^{-1}$ and $\Delta x$ is about 75 cm.

If the sea were truly described by linear theory, the mean square amplitude and slope would have been enhanced by the factors 6 and 10, respectively, at the edge of the "full wave" region. However, the time for the wave packet to travel from a point at the edge of the current region (say x = - 50 meters) to the point of maximum enhancement (the edge of the "full wave" region) is very long: $\Delta t \approx 6\ \Delta/c = 600$ seconds or about 770 wave periods. According to Figure 15, it is unlikely that such a wave will have such a long coherence time except when the wind speed is quite low. Thus it is more appropriate to ask what happens to a wave which is born within the current pattern and which travels a relatively short distance from its birth place.

Consider a wave generated at the point A in Figure 14 (26 meters beind the crest of the internal wave). Such a wave has a wavelength of 74.2 cm and a group velocity of 52.2 cm/sec (2.25 cm/sec relative to the internal wave). In 50 seconds (64 wave periods), it will move to a point 1.12 meters closer to the internal wave crest. During this time its mean square amplitude and slope will be enhanced by the factors 1.23 and 1.30 respectively. These values are probably more realistic for the normal state of the ocean than the values quoted in the previous paragraph.

It is to be noted that the enhancement effects discussed above are only one of two effects that result in modification of ocean wave spectra. Even in the absence of enhanced amplitudes, a spectrum will be altered because of the simultaneous wavenumber changes induced by the current gradient (refraction). In order to assess the simultaneous effects of these two phenomena, as well as to account for the finite coherence time effects and the effects of non-linear saturation, it is necessary to develop a formalism for treating the spectral deformation in terms of a spectral relaxation or transport equation. The development of such a model will be the subject of subsequent reports.

The spectral modifications predicted by the present model are summarized Figure 16. The phasing of the "smoothed" region (i.e., the mechanical "slicks") in this linear wave model is just opposite to that one would expect as a result of enhanced viscous damping in the convergence regions due to an accumulation of organic material or other debris.

Although one is tempted to draw conclusions concerning the phase relationship of regions of roughening and smoothing in the ocean based on this linear model, it must be remembered that the actual predicted effect is one of spectral distortion with simultaneous enhancement of some wavelengths and suppression of others. The non-linear effects present in real saturated ocean spectra are not likely to affect all wavenumbers equally. Thus the model needs to be extended to include the effects of wind generation of waves and of non-linear wave-wave interactions, including wave breaking, before one can make confident predictions of real ocean wave spectra modifications.

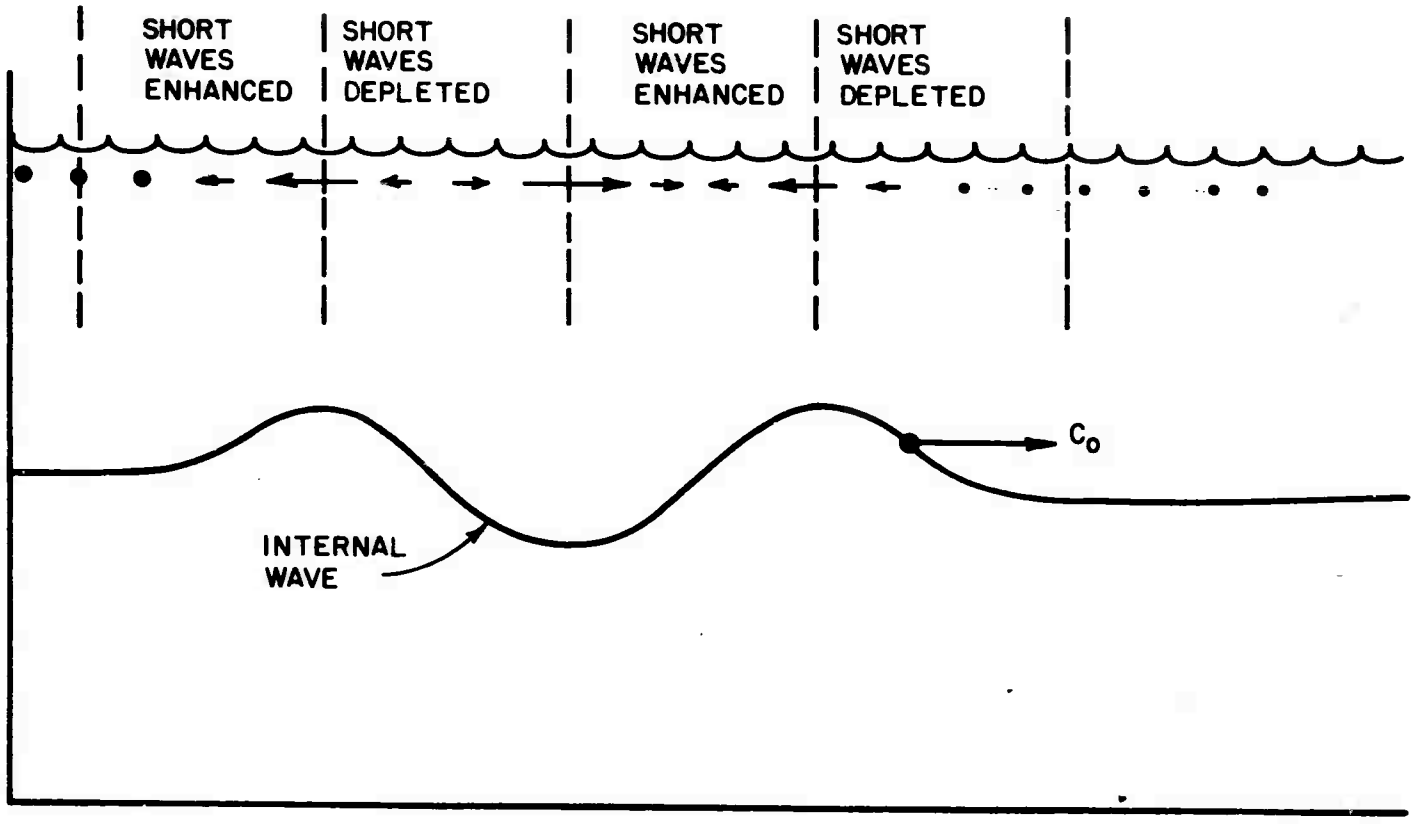


FIGURE 16. MORPHOLOGY OF MECHANICAL WAVE MODIFICATION IN A LINEAR SEA

## APPENDIX: MICRO-STRUCTURE OF THE TURNING POINT AND APPLICABILITY OF THE WKB APPROXIMATION

As pointed out in the WKB approximation of Section 4, there exists the possibility of reflected waves at the WKB turning points, i.e., the points where the wave amplitude becomes infinite. According to the dispersion relation [Equations (3.44) and (3.45)], the reduced wavenumber $\kappa$ has an imaginary part (corresponding to evanescent waves) when

$$1 - 4\eta(1-\beta) + 4\eta^2\beta^2 < 0 \quad , \tag{A.1}$$

in other words, when the reduced frequency $\eta$ lies between the critical values:

$$\eta_1 = \frac{1-\beta}{2\beta^2}\left\{1 - \sqrt{1-\beta^2/(1-\beta)^2}\right\} \tag{A.2}$$

and

$$\eta_2 = \frac{1-\beta}{2\beta^2}\left\{1 + \sqrt{1-\beta^2/(1-\beta)^2}\right\} \tag{A.3}$$

that is, when

$$\eta_1 \leq \eta \leq \eta_2 \tag{A.4}$$

the wave cannot propagate. Thus, for small values of $\beta$, evanescent waves are expected when

$$\frac{1}{\beta^2} \geq \eta \geq \frac{1-\beta}{4} \tag{A.5}$$

which is obtained by expanding Equation (A.2). Of primary interest to us is

the low frequency limit, since we learned earlier that at this limit the reflected wave amplitude becomes infinite in the WKB approximation.

To expand on this result, let us consider the group velocity of the surface wave in this (moving) coordinate system. Using the dispersion relation [Equation (5.2)] for the reduced frequency, and neglecting terms gradratic in $\beta$:

$$\eta \simeq -\kappa(1-\beta) \pm \sqrt{\kappa} \tag{A.6}$$

we obtain for the group velocity (relative to the internal wave velocity c)

$$\frac{c_g}{c} = \frac{d\eta}{d\kappa} = -(1-\beta) \pm \frac{1}{2\sqrt{\kappa}} \tag{A.7a}$$

where the upper sign corresponds to the low frequency mode of interest; thus

$$\frac{c_g}{c} \simeq -1 + \frac{1}{\sqrt{4\kappa}} + \beta \tag{A.7b}$$

and, at the point $\eta = \eta_1 \sim 1/[4(1-\beta)]$ where $\kappa \simeq 1/[4(1-2\beta)]$, the group velocit is

$$\frac{c_g}{c} \simeq -(1-\beta) + \sqrt{1-2\beta} \approx 0 \quad . \tag{A.8}$$

The point $\eta = \eta_1$ is thus a turning point and corresponds to specular or total reflection of the gravity wave by the surface current at points where $\beta \simeq 1 - 1/4$ [see Equation (4.23)].

In the evanescent region the wavenumber is complex and may be written in the form

$$\kappa = \kappa_R + i\kappa_I \tag{A.9}$$

which when substituted into the dispersion relation Equation (3.11) yields values for $\kappa_R$ and $\kappa_I$:

$$\kappa_R = \frac{1-2(1-\beta)}{2(1-2\beta)} \tag{A.10}$$

and

$$\kappa_I^2 = \frac{(1-\beta)\eta - \frac{1}{4}}{(1-2\beta)^2} \quad . \tag{A.11}$$

For small $\beta$ these expressions are $\Big|$ in terms of the critical frequency $\eta_1 = \frac{1}{4(1-\beta)}$ $\Big|$ :

$$\kappa_R \simeq \frac{1}{4}\left(1 - \frac{2\eta}{\eta_1}\right) \tag{A.12}$$

and

$$\kappa_I^2 \simeq \frac{1}{4}\left(\frac{\eta}{\eta_1} - 1\right) \tag{A.13}$$

A measure of the applicability of the WKB approximation is the relative magnitude of the "skin depth" or penetration depth at the turning point compared to the dimension of the current pattern. The penetration length is of order

$$d \sim \frac{1}{\kappa_I k^*} \quad . \tag{A.14}$$

It is convenient to evaluate this length near the resonant condition, i.e., near the value of $\kappa_R$ for which $\frac{1}{2}\sqrt{g/k^*} = c$. For an internal wave propagating along an interface at depth D between two uniform layers that differ in density by an amount $\Delta\rho$, we may write (since $c^2 = g(\Delta\rho/\rho)D$)

$$k^* = \rho/D\Delta\rho \quad . \tag{A.15}$$

Thus,

$$d \simeq 2(\Delta\rho/\rho)D \Big/ \sqrt{4\eta - 1 - \beta} \quad . \tag{A.16}$$

As $\beta$ increases, higher and higher frequencies can propagate. Thus, the negative parts of the current will reflect the lowest frequencies and the more negative is the value of the $\beta$ in the wave trough, the stronger will the extinction of the surface waves be. The value that $(-\beta)$ must exceed the critical value $(1 - 4\eta)$ in order that the penetration depth be, say, 5% or less of the thermocline depth D is given by:

$$-\beta_{5\%} = 1 - 4\eta + 0.0016 \tag{A.17}$$

where we have taken an air-water interface ($\Delta\rho/\rho = 10^{-3}$). Thus, small changes in $\beta$ will cause a wave that could just penetrate the entire current region to be reflected in quite short distances. This change is small compared to typical variations of $\beta$ expected.* Thus, for most of the waves we can assume that if they are reflected at all, they will be reflected from highly localized regions.

---

* The internal wave height $Y_I$ is given by

$$\frac{Y_I(\xi)}{D} \sim \frac{\sinh KD}{KD} \beta(\xi)$$

For the typical case $KD \lesssim 1$, significant wave heights ($Y_I > .01D$) are always associated with $\beta$ variations large compared to that in Eq. (A.17).

## REFERENCES


1. Ball, F. K., "Energy Transfer between External and Internal Gravity Waves," J. Fluid Mech. 19, 465-78 (1964).

2. Benjamin, T. B., "Instability of Periodic Wavetrains in Nonlinear Dispersive Systems," Proc. Roy. Soc. A, 299, 59 (1967).

3. Hartle, J. B. and F. Zachariason, Institute for Defense Analyses Study S-334, Vol. II, pp. 69-82 (April, 1969).

4. Hasselman, K., "Nonlinear Interactions Treated by the Methods of Theoretical Physics (with application to the generation of waves by wind)," Proc. Roy. Soc. A, 299, 77-100, (1967).

5. Holliday, D., "Change in Surface Wave Roughness induced by Internal Waves," R & D Associates Report No. RDA-TR-004 (July 1971).

6. Lafond, E. C. in The Sea, Vol. 1, pp 731-751, Interscience Publishers, (1962).

7. Longuet-Higgins, M.S. and R. W. Stewart, "The Changes in Amplitude of Short Gravity Waves on Steady Non-uniform Currents," J. Fluid Mech. 10, 529-49, (1961).

8. Perry, R. B. and G. R. Shimke, "Large Amplitude Internal Waves Observed off the Northwest Coast of Sumatra," J. Geophys. Res. 70, 2319 (1965).

9. Phillips, O. M., The Dynamics of the Upper Ocean, Cambridge University Press, (1966).

10. Phillips, O. M., "Surface Wave Effects Produced by Internal Waves," Hydronautics Technical Report No. 7015-3.

11. Polvani, D. G., "Final Report for the NURDC Tower Experiment," Westinghouse Electric Corporation (June 1972).

12. Rosenbluth, M., "Surface Waves in the Presence of an Internal Wave," Institute for Defense Analyses Report No. P-832 (Nov. 1971).

13. Whitham, G. B., "A General Approach to Linear and Non-linear Dispersive Waves using a Lagrangian," J. Fluid Mech. 22, 273-83, (1965).